Dynamics of Ramp-Initiated Reactor Transients

G. Kußmaul
Institut für Neutronenphysik und Reaktorphysik
Projekt Nukleare Sicherheitsforschung

Kernforschungszentrum Karlsruhe
Institut für Neutronenphysik und Reaktortechnik
Projekt Nukleare Sicherheitsforschung

KfK 5352

DYNAMICS OF RAMP-INITIATED
REACTOR TRANSIENTS

Günter Kußmaul

Kernforschungszentrum Karlsruhe GmbH, Karlsruhe

Abstract

Transients in nuclear systems induced by reactivity ramps develop different types of power traces - exponential, single-pulse, oscillating - depending on the ramp rates and the neutron lifetime of the system. Starting from the kinetics equations of the point reactor and using a model of energy-dependent feedback reactivity, based on the prompt and inherent Doppler effect, simple relations for the dependence of energy release and power shape on ramp rate, energy coefficient and neutron lifetime are derived. Depending on neutron lifetime of the nuclear system the ranges of ramp rate are determined, which define the type of power trace. In the regime of superprompt-critical transients, the models of step and ramp insertions are especially investigated. The ranges of applicability have been checked by comparison with calculations using the dynamics code system DYANA2 which solves numerically the set of kinetics and thermal-hydraulics equations describing different feedback loops. This comparison shows that these relations are useful in their restricted regime of application for qualitative discussion and a physical understanding of the phenomena. For quantitative results, however, coupled kinetics/thermal-hydraulics codes like DYANA2 have to be used.

Zur Dynamik von Reaktortransienten bei rampenförmiger Reaktivitätszufuhr

Zusammenfassung:

Bei Reaktortransienten, die von Reaktivitätsrampem ausgelöst werden, können, je nach Rampenstärke und Neutronenlebensdauer, unterschiedliche Typen von Leistungsverläufen auftreten - exponentieller Anstieg, Einzelpuls oder Oszillationen. Ausgehend von den kinetischen Gleichungen des Punktreaktors und einem auf dem prompten, inhärenten Dopplereffekt beruhenden energieabhängigen Modell für die Reaktivitätsrückführung, werden einfache Beziehungen hergeleitet, die die Abhängigkeit der Energiefreisetzung und des Leistungsverlaufs von Rampenstärke, Energiekoeffizient und Neutronenlebensdauer darstellen. Insbesondere werden die beiden Fälle mit sprung- und rampenförmiger Reaktivität im Bereich superprompt-kritischer Transienten untersucht. Die Wertebereiche der Rampenstärke, die den Typ des Leistungsverlaufs bestimmt, werden in Abhängigkeit von der Neutronenlebensdauer ermittelt. Um den Anwendungsbereich eines jeden dieser Modelle zu ermitteln, wurden Rechnungen mit dem Programmsystem DYANA2 ausgeführt, welches das Gleichungssystem, bestehend aus den kinetischen Gleichungen des Punktreaktors und thermohydraulischen Gleichungen zur Bestimmung der verschiedenen Reaktivitätsrückführungen, numerisch löst. Der Vergleich ergab, daß die einfachen Beziehungen in ihrem jeweiligen Anwendungsbereich eine nützliche Grundlage für eine qualitative Diskussion und für ein physikalisches Verständnis der Phänomene liefern. Für quantitative Zusammenhänge ist jedoch die Berechnung mit einem dynamischen Programm wie DYANA2 erforderlich.

Table of Contents

I. Introduction

The transient behaviour induced in power reactors by accidental insertions of reactivity is strongly dependent on the rate and magnitude of the insertion as well as the design characteristics of the reactor and the state of the system at the time of the accident. In fast transients, control and shutdown devices are likely to be too slow to have an appreciable effect in limiting the transient. In such situations it is vitally important for the safety of nuclear reactors to have a prompt and inherent feedback available. Without it, the neutron flux would rise so rapidly in the case of a superprompt-critical excursion that mechanical shutdown devices could not reduce the power before it reaches destructive levels. The Doppler broadening of resonances - through reduction in resonance self-shielding - is directly associated with the fuel temperature and leads to an increase in neutron absorption and thus to a prompt, negative and inherent reactivity feedback. It is fundamental to the design because of physical laws and thus totally reliable.

A systematic study of transients is facilitated by dividing reactivity accidents into broad categories according to the time-dependence of the initiating reactivity $\rho_i(t)$. Approximating the initiating reactivity by the ramp

$$\rho_i(t) \;=\; \begin{Bmatrix} \dot{\rho}\, t \\ \dot{\rho}\, t_0 \end{Bmatrix} \quad \text{for} \quad \begin{Bmatrix} 0 \le t \le t_0 \\ t > t_0 \end{Bmatrix},$$

the insertion is characterized by a ramp rate $\dot{\rho}$ (in s^{-1}) and a magnitude, $\dot{\rho} t_0$. If the initial power level is orders of magnitudes below the range where operation at power takes place, a very fast reactivity insertion may be completed before the power reaches the level where temperature and density changes begin to cause reactivity feedback. If, in addition, the insertion is completed before a power level, that will cause the shutdown system to be actuated, is reached, the reactivity insertion may be approximated as an instantaneous step insertion. In these cases, the magnitude of the reactivity determines the transient behaviour. At higher power levels the ramp rate has to be considerably faster to attain these conditions. This may, however, still be a valid approximation for thermal systems due to their slower kinetics behaviour.

In fast systems or at initial power levels which are closer to the operating level, prompt reactivity feedback will follow immediately from the power changes accompanying the insertion. In these situations it is the rate of reactivity insertion, $\dot{\rho}$, that becomes of primary importance. The maximum total reactivity that is reached during the accident is more closely related to the ramp rate, $\dot{\rho}$, than to the reactivity magnitude, $\dot{\rho} t_0$.

When reactivity is added while the reactor is at power, the feedback and the control system tend to compensate for the insertion. If the ramp rate is slow compared to the thermal time constant of the core, the delayed neutron behaviour and the control system response time, the reactor slowly passes through a sequence of near-equilibrium conditions in which power and temperature distribution are essentially the same as those during steady state operation. These transients are called *quasi-static*.

If we consider increasingly faster rates of reactivity insertion, feedback and control reactivity can no longer respond fast enough to compensate for the reactivity insertion. The properties of delayed neutrons then become important in deter-

mining the neutron kinetics of the transient. The transient is now likely to take place on a time scale that is comparable to the time required to remove heat from fuel to coolant. The fuel temperature is then governed by transient heat conduction and convection. This complex interaction of neutron kinetics and transient heat transfer is typical of transients for which the net reactivity rises well above zero but does not reach prompt critical. This type of transients are often called *superdelayed-critical transients*.

Transients, for which reactivity is added so fast that the net reactvity rises above prompt critical before reactvity reduction mechanisms - essentially prompt feedback reactivity - become effective in reducing the reactivity, are called *super-prompt-critical transients*. The reactor period becomes so short that delayed neutrons no longer play an important role and the neutronic behaviour is governed by the prompt-neutron generation. Moreover, heat transport out of the fuel is not very important on these short time scales, and the fuel may be assumed to exhibit an essentially adiabatic thermal behaviour.

The mechanisms by which transients are terminated vary considerably as one passes from quasi-static to superdelayed-critical and from superdelayed-critical to superprompt-critical reactivity accidents. Whether the safety system is able to terminate a transient before destructive levels are reached depends on the transient time between the initiating event and the time at which the protection system detects unacceptable changes in the state of the reactor as well as on the inertial delays of the shutdown system, i.e. the time between the actuation of the shutdown system and the termination of the chain reaction by the control rods. On the relatively long time scales of quasi-static transients the additional power produced during the inertial delays has a negligible effect on the reactor core. With the more rapid rates of power increase, typical for superdelayed-critical transients, the power produced during the inertial delays may be a significant fraction of the total energy release. Superprompt-critical transients occur on such short time scales that only a prompt inherent reactivity feedback (Doppler effect) is able to terminate the power burst.

The critical parameters on which fuel damage depends also change as one goes from very slow to very fast reactivity transients. In quasi-static transients the maximum fuel temperature is determined by the maximum power level, P_{max}, that is reached before the transient is terminated. For superdelayed-critical transients, transient heat transport has to be taken into account to relate the maximum fuel temperature to the power history. With the very fast transients that characterize superprompt-critical reactivities, the adiabatic thermal behaviour leads to fuel temperatures which are proportional to the total energy release.

If in any of the preceding situations the fuel melting point is reached, the energy release is consumed to melt fuel instead of increasing the fuel temperature and the fuel enthalpy rather than the temperature determines what fraction of the fuel will melt. In extremely severe superprompt-critical transients the fuel may not only melt but even vaporize and generate destructive effects by high pressure. Since this takes only place when the energy release rate is so fast that the pressure cannot be dissipated by expansion of surrounding materials, the maximum power again becomes an indication of the destructiveness of the burst.

In the following section the theoretical basis of the mathematical treatment of transients is considered, starting from the kinetics equations of the point reactor.

Then, different feedback components are analyzed with special emphasis of the prompt and inherent Doppler effect. In the remaining part of the section, the special cases of step and ramp reactivity insertions are treated in order to find simple relations for the dependence of power and energy release on characteristic core and accident parameters like neutron generation time, energy coefficient, ramp rate and reactivity magnitude. A whole series of transients with ramp insertions of different rates was calculated for reactor systems with different values of prompt-neutron generation time using the dynamics code DYANA2 to demonstrate the validity and the applicability of these simplified models.

II. Theoretical Considerations

II.1. The Kinetics Equations of the Point Reactor

The kinetics equations of a point reactor in the source-free case are usually written as follows [1]

$$\frac{dn}{dt} = \frac{\rho(t) - \beta}{\Lambda} n(t) + \sum_{i=1}^{N} \lambda_i C_i(t) \tag{1}$$

$$\frac{dC_i}{dt} = \frac{\beta_i}{\Lambda} n(t) - \lambda_i C_i(t), \quad (i = 1, ... N) \tag{2}$$

where
  $n(t)$ = neutron density (neutrons/cm^3) at time t,
  $C_i(t)$ = ith delayed-neutron group precursor density (precursors/cm^3) at time t,
  N = number of delayed neutron groups (N = 6 for each fissionable nuclide),
  β_i = effective fraction of the ith group of delayed neutrons,
  $\beta = \sum_{i=1}^{N} \beta_i,$

  λ_i = decay constant of the ith group of delayed-neutron precursors (s^{-1}),
  $\rho(t)$ = (k - 1)/k = reactivity at time t,
  k = multiplication constant,
  Λ = prompt-neutron generation time (s).

The prompt-neutron generation time Λ (which measures the neutron birth-to-birth time) is related to the neutron lifetime ℓ (which measures neutron birth-to-death time) as follows:

$$\ell = k \Lambda. \tag{3}$$

This relationship implies that ℓ exceeds Λ when the power is rising (k > 1) and that Λ exceeds ℓ when the power is decreasing (k < 1). Because k is always very close to unity, even for large postulated accident conditions, both terms are loosely referred to as neutron lifetime. (For technical reasons, ℓ is used in the figures instead of Λ). The dimensionless reactivity ρ is often expressed in units of dollars ($) which is obtained by dividing the absolute value of ρ by β.

For many safety calculations it is convenient to change the principal variable in the kinetics equations from neutron density, n, to reactor power, P (in W). This can be done by first converting neutron density to fission rate, then multiplying

3

with the energy release per fission ($\approx$213 MeV) and finally integrating over the whole reactor volume. There is, however, the complication that fission takes only place in fuel, but energy is also absorbed throughout the reactor through gamma rays and neutrons. The gross space distribution of energy deposition by gamma rays and neutrons differs from that of fission fragments and beta particles which remain in fuel. Therefore only about 95 % of the total energy is released in fuel at steady state operation and only part of the energy (about 94%) is promptly released, the rest is released with delay in the form of beta particles and gamma rays at the time of fission product beta decay. This effect is only important in rapid transients, but then it results that only about 90% of the total stationary energy is released in fuel. The treatment of this complication is beyond the scope of this study.

It is convenient to separate the reactor power, $P(t)$, into the nominal power, P_n (usually called "full power", abbreviated "fp"), and the flux amplitude function, $p(t)$:

$$P(t) \simeq P_n p(t). \tag{4}$$

The "$\simeq$" sign needs to be used since p(t) describes only approximately the amplitude of the power. In this approximation then, the value p_0 represents the ratio of initial to nominal power.

With this variable, the kinetics equations (Eqs. (1) and (2)) become

$$\frac{dp}{dt} = \frac{\rho(t) - \beta}{\Lambda} p(t) + \sum_{i=1}^{N} \lambda_i c_i(t) \tag{5}$$

$$\frac{dc_i}{dt} = \frac{\beta_i}{\Lambda} p(t) - \lambda_i c_i(t), \quad (i = 1, ... N) \tag{6}$$

where c_i is a corresponding power contribution from the ith group of delayed-neutron precursors.

These equations are the basis for most kinetic investigations. It is assumed that the kinetic parameters Λ and β_i as well as the flux shape are time-independent. Under special conditions for the reactivity, the Eqs. (5) and (6) can be solved analytically. In the general case of time-dependent reactivity, however, the kinetics equations must be solved numerically.

II.2. Instantaneous Reciprocal Period

In kinetics studies it is often useful to characterize the dynamic behaviour by the instantaneous reciprocal period

$$\alpha(t) \equiv \frac{\dot{p}(t)}{p(t)}. \tag{7}$$

If $\alpha(t)$ is known, major response characteristics are uniquely determined. Thus $p(t)$ is given by

$$p(t) = p_0 \exp\left[\int_0^t \alpha(t')\, dt'\right] \tag{8}$$

and the reactor power $P(t)$ by Eq. (4). Similarly the total energy release in an excursion is also determined when $\alpha(t)$ is specified:

$$E(t) \simeq P_n \int_0^t p(t')\, dt'. \tag{9}$$

A useful expression for $\alpha(t)$ can be obtained from Eqs. (5) and (6) as shown in *Appendix 1*:

$$\alpha(t) = \frac{\rho(t)}{\Lambda} - \frac{\beta}{\Lambda} \sum_{i=1}^{N} \frac{a_i}{1 + \dfrac{\lambda_i}{\dot{c}_i/c_i}}, \tag{10}$$

where $a_i = \beta_i/\beta$.

If reactivity is added as a ramp and if there is no system feedback we have

$$\rho(t) = \dot{\rho}\, t \tag{11}$$

where $\dot{\rho}$ is constant. $\alpha(t)$ will now increase with time and will ultimately approach the value

$$\alpha(t) = \frac{\rho(t) - \beta}{\Lambda} \tag{12}$$

since $\dot{c}_i/c_i \gg \lambda_i$. This is the familiar "prompt-α", observed after a sudden change of reactivity, and it governs the kinetic behaviour of a system sustained by prompt neutrons alone.

In the case of enormous reactivity addition, $\dot{\rho} \gg \beta/\Lambda$, no time is available for precursor formation, and the theoretical limiting α is given by

$$\alpha(t) = \frac{\rho(t)}{\Lambda} \tag{13}$$

(cf. dashed curves in Fig. 1). Typical values of β/Λ for Pu-fuelled systems with neutron generation times of 10^{-6} and 10^{-4} s are 3400 and 34 s^{-1}, respectively.

For very small rates of reactivity addition ($\dot{\rho} \to 0$), $\alpha(t)$ approaches a steady value, $\alpha \to T^{-1}$, where T is the stable reactor period. Under this condition of constant α, Eq. (10) becomes

$$\alpha \equiv T^{-1} = \frac{1}{\Lambda}\left(\rho - \beta \sum_{i=1}^{N} \frac{a_i}{1 + \lambda_i T}\right) \tag{14}$$

5

which is the characteristic ("Nordheim") relation between reactor period and reactivity.

Eqs. (13) and (14) determine the upper and lower limit of the values of α. For intermediate values of ramp rate, the kinetics equations must be solved numerically for instantaneous $\alpha(t)$. Such solutions have been obtained by the RTS code [2] for various ramp rates and prompt-neutron generation times in the case of a U^{235}-fuelled system. Fast reactors have a smaller value of β, therefore the upper limit, Eq. (13), is correspondingly smaller. For a qualitative discussion, three figures from [2] are reproduced here. Fig. 1 shows the values of $\alpha(t)$ for the limiting cases, i.e. Eqs. (13) and (14), as well as for a ramp of 1000 $/s as a function of reactivity for various prompt-neutron generation times. Values of instantaneous $\alpha(t)$ for intermediate ramp rates between 0 and 1000 $/s are plotted in Figs. 2 and 3 for $\Lambda = 10^{-4}$ and 10^{-6} s, respectively.

The plots of Figs. 2 and 3 are very useful for the interpretation of power traces caused by ramp insertion (see Section III). It should be emphasized that reactivity feedback effects have been neglected in the discussion above. A complete analysis of the dynamic response must include feedback; this subject is treated in the remaining part of Section II.

II.3. Reactor Dynamics

In the previous paragraph the time behaviour of a reactor has been considered under the only condition of insertion of reactivity which was assumed to be independent of the operating conditions. This is useful so long as the power level in the reactor is very low. However, as soon as power is produced at a level sufficient to cause significant temperature rises in fuel, coolant, and other core constituents, the assumption of power-independent reactivity is no longer valid. As a consequence, material densities and microscopic cross sections in the reactor are affected. Since the multiplication of the core depends on these quantities, a reactivity feedback loop is established in which $\rho(t)$ is dependent on temperatures and densities that are determined, in turn, by reactor power history and heat transport in the core. If feedback is involved, the system of kinetics equations, Eqs. (5) and (6), must be supplemented by another set of equations describing the various feedback loops. This extended system of coupled equations is often designated as the reactor dynamics equations.

The complex interplay between neutron chain reaction, thermal hydraulics reactivity feedback, and reactor control and shutdown system is frequently replaced by a simple lumped parameter model, which tends to be less accurate but often provides a better physical insight into the nature of the various feedback phenomena. By neglecting the control and shutdown system for this investigation, the reactivity is represented in this model in a compact form by

$$\rho(t) = \rho_i(t) + \rho_{fb}(t) \tag{15}$$

where $\rho_i(t)$ is the reactivity caused by the initiating event (reactivity insertion) and $\rho_{fb}(t)$ is the reactivity from feedback.

In fast reactors heat is produced approximately uniformly across the fuel region (pin) and transported radially outward through the fuel, across the fuel-cladding gap, through the cladding, and into the coolant channel. It is then carried away

by coolant convection parallel to the fuel element axis. The model assumes that these thermal hydraulic phenomena can be approximated by relatively few variables [3]. Most often, these are fuel temperature (T_f), coolant temperature (T_c), and coolant inlet temperature (T_i). Reactivity feedback changes may be represented in terms of these temperatures as

$$\delta\rho_{fb} = \left(\frac{\partial\rho}{\partial T_f} \right) \delta T_f + \left(\frac{\partial\rho}{\partial T_c} \right) \delta T_c + \left(\frac{\partial\rho}{\partial T_i} \right) \delta T_i. \qquad (16)$$

In the general case, T_f and T_c depend on radial and axial position in the core. In dynamics codes, e.g. DYANA2, they are calculated locally and simultaneously with power and reactivity during the course of a transient. Integrating the worth-weighted incremental feedback contributions, obtained locally from Eq. (16), over the whole reactor, gives the total feedback reactivity which is inserted into Eq. (15).

The temperature coefficients of reactivity

$$\left(\frac{\partial\rho}{\partial T_x} \right), \qquad x = f, c, \text{ or } i$$

may be obtained experimentally from measurable composite coefficients or from neutronics code calculations.

In even more simplified models of power reactor dynamics, the temperatures in Eq. (16) are core-averaged values. In general, this requires again modelling the thermal transient with the use of coupled sets of differential equations in time, simultaneously with the solution of the kinetics equations. However, there are special situations for which simple relations can be derived for core-averaged temperatures and a single independent variable can be used to deduce a global coefficient.

II.4. Prompt Reactivity Coefficient

Temperature changes which occur in a transient are characterized by different time constants. Heat is produced in the fuel, transferred to the coolant by heat conduction and transported to the heat exchanger by the coolant flow. Changes of core inlet temperature T_i are characterized by the time necessary for the coolant to return to the core inlet after having passed through the primary loop. This takes many tens of seconds or even minutes, depending on the system and the flow rate. The heat transfer from fuel to coolant is faster, but still has a time constant of several seconds, mainly determined by fuel heat conductivity. In the event of a very large reactivity insertion, the reactor power may change significantly over periods of time that are short compared to that required to transfer heat from fuel to coolant. Over such time periods the coolant temperature does not change appreciably, all the more so the coolant inlet temperature, and the only reactivity effect comes directly from the heating of the fuel. Hence we assume $\delta T_c = \delta T_i \simeq 0$, and obtain from Eq. (16) in differential form

$$d\rho_{fb} = \left(\frac{\partial\rho}{\partial T_f} \right) dT_f. \qquad (17)$$

7

The problem is now to find a relation between energy release and fuel temperature rise. If transients start from a steady state power level P_0, the power $P(t)$ can be split into the stationary component P_0 and the power increment $\delta P(t)$:

$$P(t) = P_0 + \delta P(t). \tag{18}$$

During rapid transients most of the energy that is deposited in fuel raises the fuel temperature. Heat transfer to the cladding and coolant can be either completely neglected or taken partly into account. There are therefore two different approximations to describe the fuel temperature increase: (i) the completely adiabatic fuel or (ii) the adiabatic fuel for the power increment [1]. In the first case it is assumed that

$$dT_f \propto \int_0^t P(t')dt' \tag{19}$$

and in the second case that

$$dT_f \propto \int_0^t \delta P(t')dt' = \int_0^t (P(t') - P_0)\, dt'. \tag{20}$$

The use of the first model, often called "linear energy" model, is physically not well justified in most transients, but it greatly simplifies the mathematical treatment. It is for instance used to deal with step reactivity insertions or if the transient starts from zero power level. The second model can be applied for ramp-induced excursions because the stationary term is equivalent to a positive reactivity ramp insertion and can be easily considered.

If M_f is the total mass of fuel in the core and c_f is the fuel specific heat per unit mass, we have with the completely adiabatic boundary condition

$$M_f c_f\, dT_f = P(t)\, dt$$

or

$$dT_f = C_P\, P(t)\, dt \tag{21}$$

where

$$C_P \equiv \frac{1}{M_f c_f}$$

is the conversion factor between energy release and fuel temperature rise, expressed in units of K/(Ws). Combining Eqs. (17) and (21), we obtain

$$d\rho_{fb} = \mu\, P(t)\, dt. \tag{22}$$

The quantity

$$\mu \equiv C_P \left(\frac{\partial \rho}{\partial T_f} \right)$$

is often referred to as prompt reactivity coefficient or more explicitly as prompt energy coefficient of reactivity. The unit is either (Ws)$^{-1}$ or \$/(Ws), if the reactivity is expressed in units of \$. Reactor cores must be designed so that μ has a nega-

8

tive value, for a positive prompt coefficient would lead to inherently unstable systems that could undergo autocatalytic excursions.

In all applications where the Eqs. (5) and (6) are used, the power is separated according to Eq. (4) and instead of Eqs. (21) and (22) we obtain the following relations (distinguished by minuscule p from majuscule P):

$$dT_f = C_p \, p(t) \, dt \tag{23}$$

and

$$d\rho_{fb} = \gamma \, p(t) \, dt \tag{24}$$

with the corresponding energy-to-temperature conversion factor

$$C_p \equiv \frac{P_n}{M_f \, c_f} \tag{25}$$

and the prompt energy coefficient

$$\gamma \equiv C_p \left(\frac{\partial \rho}{\partial T_f} \right). \tag{26}$$

If C_p and γ are temperature independent, then the Eqs. (23) and (24) can be integrated and we obtain for the fuel temperature rise

$$\Delta T_f = C_p \, I(t) \tag{27}$$

and for the feedback reactivity with $\rho_{fb}(0) = 0$ and assuming $\gamma < 0$:

$$\rho_{fb}(t) = - |\gamma| \, I(t). \tag{28}$$

We have used the integral

$$I(t) = \int_0^t p(t')dt' \tag{29}$$

which describes the energy in units, which are called here "relative full-power seconds" (fp-s). C_p is the corresponding factor between energy release and fuel temperature rise, expressed in units of K/(fp-s), and γ is the corresponding prompt energy coefficient of reactivity in units of either (fp-s)$^{-1}$ or \$/(fp-s), respectively.

An estimate of the energy conversion factor C_p for EFR can be made by assuming for the average power density a value of $P_n/ M_f = 70$ W/g and taking the temperature dependent values for c_f as used in the dynamics code DYANA2, described in Sect.III.2 and shown in Fig. 4. The resulting values for C_p are plotted in Fig. 5. The temperature rise caused by an energy release of 1 fp-s is about 200 K at the lower end of fuel temperatures and decreases to about 100 K near the fuel melting temperature of 2645 °C. The energy-to-melt corresponds to about 10 fp-s for transients from 0.2 fp.

Generally, light water reactors have smaller values of power density (20 to 40 W/g). Fig. 5 shows the values for a light water-moderated core (CABRI reactor) with a power density of 23.2 W/g. In this case, the temperature rise due to an energy release of 1 fp-s is only about 50 K and the energy-to-melt is about 3 to 4 times higher than in fast reactors. The power density is even smaller in gra-

phite-moderated reactors with values between 2 and 12 W/g [4]. Values for γ will be shown in the following section where the Doppler coefficient is treated to some detail.

II.5. Doppler Coefficient

There is only one really prompt feedback effect in thermal as well as fast reactors, namely the Doppler effect. The corresponding feedback loop is as short as possible since the Doppler broadening of resonances occurs simultaneously with the dissipation of the kinetic energy of the fission products in the fuel. The axial expansion is the other feedback effect which may be considered as prompt in most transients. The fuel temperature rise does not directly cause this reactivity feedback, but is only the source of a force. Two further time integrations are required to obtain the axial displacement and the corresponding fuel density reduction that causes the reactivity. The displacement is established almost at the speed of sound in the fuel material (typically $\approx$ 1000 m/s); the corresponding delay is then $\approx$ 1ms. This delay can be neglected in most transients. The energy coefficient is then the sum of two components, the Doppler effect (γ_D) and the radial expansion (γ_{exp})

$$\gamma = \gamma_D + \gamma_{exp}.$$

The expansion coefficient is essentially independent of temperature. The Doppler reactivity effect is negative but small in metal-fuelled cores; it is larger in thermal and oxide-fuelled fast reactors due to the softer neutron spectrum. It represents the most important inherent shutdown mechanism and thus helps to assure the safety of nuclear reactors. The temperature dependence of the Doppler coefficient $\left(\frac{\partial \rho}{\partial T} \right)_D$, shows approximately a $1/T^x$ behaviour [1,5]:

$$\left(\frac{\partial \rho}{\partial T} \right)_D = \frac{A_D}{T^x}. \tag{30}$$

For oxide-fuelled fast reactors, x is very close to 1.0. For a reactor with a much harder neutron spectrum, such as metal-fuelled fast reactors, x is close to 3/2 and for a reactor with a much softer spectrum, such as a light water reactor, x is close to 1/2. The DYANA2 code uses a two-term coefficient

$$\left(\frac{\partial \rho}{\partial T} \right)_D = \frac{1}{T} \left(A_D + \frac{B_D}{\sqrt{T}} \right).$$

If the Doppler coefficient is proportional to 1/T, as in large oxide-fuelled fast reactors, a "Doppler constant", $A_D = T \left(\frac{\partial \rho}{\partial T} \right)_D$, can be introduced. Its values are in the range of

$$0.003 \lesssim |A_D| \lesssim 0.009.$$

With these values for the Doppler constant, the Doppler coefficient for an approximate average fuel temperature in an operating fast reactor (T = 1500 K) is

$$2 \times 10^{-6}/K \lesssim \left| \left(\frac{\partial \rho}{\partial T_D} \right) \right| \lesssim 6 \times 10^{-6}/K$$

or

$$0.6 \times 10^{-3} \$/K \lesssim \left| \left(\frac{\partial \rho}{\partial T_D} \right) \right| \lesssim 1.8 \times 10^{-3} \$/K.$$

The Doppler effect in thermal systems is larger than in fast systems because (i) the enrichment is smaller and therefore the atom density of fertile material in the fuel is larger and (ii) the neutron spectrum is shifted downward in energy, causing a higher fraction of neutrons to be in the energy range of the cross section resonances. For comparison, at 1500 K the CABRI core has a Doppler coefficient of $13 \times 10^{-6}/K$ or more than twice the upper value of a fast reactor, but the higher value of β, e.g. 678×10^{-5} in the U^{235}-fuelled CABRI core [6], reduces the corresponding value to 1.9×10^{-3} $/K.

A decrease in the amount of light or intermediate atomic weight material in a fast reactor core causes a decrease in neutron slowing down due to elastic scattering collisions, and this, in turn, results in a hardening of the neutron energy spectrum. The loss of coolant in a sodium-cooled fast reactor results therefore in a decrease of the Doppler coefficient.

The Doppler component of the prompt energy coefficient, γ_D, is plotted in Fig. 6 for EFR and CABRI. The reduction with temperature is considerable in the case of a fast reactor. It is somewhat smaller in thermal cores due to the slower reduction of the Doppler coefficient with temperature. It is evident from Fig. 6 that a higher energy release is necessary in thermal reactors in order to produce the same amount of feedback reactivity in terms of $.

II.6. Superprompt-critical Excursions

Dramatic changes take place in the nature of reactivity accidents as one passes from transients for which $\rho_{max} < \beta$ to superprompt-critical excursions for which $\rho_{max} > \beta$. As indicated in Fig. 1, the instantaneous inverse period increases by as much as several orders of magnitude for fast systems as the reactivity passes through prompt critical. For slower systems the transition to superprompt-critical is more moderate. As a result the reactor power level increases so rapidly that the reactor shut down system is ineffectual in terminating the transient. Only prompt inherent feedback mechanisms as the Doppler effect are adequate to terminate the power rise before fuel damage can occur. A typical feature of the transition to superprompt-critical is the appearance of a power burst shape (see Fig. 11).

The duration of the power burst is short compared to the thermal time constant of the core, therefore the thermal-hydraulic feedback loop can be replaced by the assumption that the core behaves completely adiabatically. Assuming that the prompt coefficient is negative and using the "linear energy" model for the feedback reactivity (cf. Eq. (28)), we obtain for the reactivity

$$\rho(t) = \rho_i(t) - |\gamma| \int_0^t p(t')dt'. \tag{31}$$

Since the burst width is short compared to the delayed-neutron precursor half-lives, the time behaviour is determined by the prompt neutrons alone. The com-

11

plete neglect of the delayed neutrons in Eq. (5) leads to the following differential equation

$$\dot{p}(t) = \frac{\rho_p(t)}{\Lambda} p(t) \tag{32}$$

where, for convenience, the prompt reactivity is designated by a single quantity

$$\rho_p(t) = \rho(t) - \beta.$$

This is called prompt kinetics approximation since only prompt-neutron multiplication is considered. This approximation holds only in the super-prompt critical domain. Applications below prompt critical may lead to physically unrealistic results.

There is some arbitrariness in the initial conditions at $t = 0$, i.e. at the time when the reactivity passes from delayed critical to prompt critical. By definition we have $\rho_p(0) = 0$ and, according to Eq. (32), $\dot{p}(0) = 0$, whereas in reality the power rises already during the delayed-critical phase of the transient and therefore the slope is positive when passing to prompt critical and the power level, $p(0)$, itself depends on the reactivity history. The prompt kinetics model may be improved, without adding any complication to Eq. (32), if the delayed neutrons are taken into account by just modifying the initial power value, $p(0)$. These so-called "pseudo-initial" conditions can be derived for idealized transients that follow step or ramp reactivity insertions. In these special cases, the Eqs. (31) and (32) can be treated analytically.

II.6.1. Step Insertions

Although step insertions are not very realistic, especially in fast systems - except when extremely rapid insertions are made at very low power levels -, they provide a good deal of insight into the nature of power bursts [1,3] initiated by ramp insertions. For purposes of comparing results from different reactor types and from more severe accidents, it is desirable to have available simple expressions that relate maximum power and energy release to insertion magnitude, prompt-neutron generation time and prompt reactivity coefficient.

The step insertion approximation starts with the reactivity

$$\rho_i(t) = \rho_0, \quad \text{for } t > 0$$

where $\rho_0 > \beta$ is the magnitude of the step insertion. The prompt reactivity is then

$$\rho_p(t) = \rho_0 - \beta - |\gamma| \int_0^t p(t')dt' \tag{33}$$

if Eq. (31) is inserted. The pseudo-initial power is in this case [1]

$$p(0) = p^0 = \frac{\rho_0}{\rho_0 - \beta} p_0 \tag{34}$$

where p_0 is the steady state value before the step.

Eq. (33) together with the initial conditions are used in the prompt kinetics approximation. Some simple theoretical relations can be derived by investigation of these equations. Insertion of Eq. (33) into Eq. (32) and division by p(t) leads to Eq. (12) and the instantaneous inverse period, $\alpha(t)$. After the onset of a transient, the power rises, but the feedback term reduces the value of $\alpha(t)$ until it becomes zero. This is where the peak power is reached at $t = t_{max}$. At this time, the prompt part of the inserted reactivity is just compensated by the feedback

$$\rho_0 - \beta = |\gamma| \int_0^{t_{max}} p(t)dt. \tag{35}$$

Note the important fact that the energy release in the first half-pulse up to peak power is independent of the prompt-neutron generation time. It only depends on the prompt excess of the injected reactivity, $\rho_0 - \beta$, and the prompt energy coefficient, γ.

Further information is obtained by considering the first integral of the Eqs. (32) and (33). This is shown in *Appendix 2*. The results are shortly discussed here. The value of power rise is according to Eq. (A.2.9)

$$p_{max} - p^0 = \frac{(\rho_0 - \beta)^2}{2\Lambda|\gamma|} \tag{36}$$

and the energy release (in units of fp-s) is (see Eq. (A.2.18))

$$I(t = 2t_{max}) = 2 \int_0^{t_{max}} p(t)dt = 2\frac{(\rho_0 - \beta)}{|\gamma|}. \tag{37}$$

If the pulse width Γ is defined by the power integral divided by the peak value, I/p_{max}, we obtain in the case $p_{max} \gg p^0$:

$$\Gamma \simeq \frac{4\Lambda}{\rho_0 - \beta}. \tag{38}$$

The proportionality of Γ to Λ, as a consequence of the Λ-independent energy production, compensates the $1/\Lambda$-dependence of p_{max}. The power rise, $p_{max} - p^0$, in Eq. (36) is independent of the initial value p^0.

From these relations we see that both, peak power and energy release, increase with the prompt excess and are inversely proportional to the prompt reactivity coefficient. The energy release is independent of the prompt-neutron generation time, however, as it is for delayed supercritical transients, and none of the parameters depends on the initial power level of the reactor, provided it is small. Thus, although the differences in reactivity insertion mechanisms and feedback effects in thermal and fast reactors are important to the characteristics of reactivity accidents, the difference in prompt-neutron generation time, per se, is not significant insofar as energy release is concerned. With decreasing Λ the peak power increases and the pulse width becomes smaller, but the energy release remains the same. If transients are considered for which the primary damage depends on the maximum power, however, the small value of Λ in fast reactors is detrimental.

The results given in Eqs. (36) to (38) were derived under the assumption of the prompt kinetics approximation, i.e. by neglect of the delayed neutron source, except as a modification of the initial condition. They describe the behaviour of the reactor during its prompt critical phase quite reasonably, but give completely unrealistic values in the post-burst phase where the power is eventually determined by the source multiplication of the delayed neutrons. Therefore the conclusions apply only to excursions for which the initial reactivity is greater than 1 $ and only during the pulse. In the real case, the power burst ends with a long tail caused by the delayed neutrons. If the step insertion is less than 1 $, the distinct prompt burst does not appear and the resulting transient is much milder, occurring over a longer time span with smaller power and energy release.

II.6.2. Ramp Insertions

Reactivity steps in the superprompt-critical domain of reactors, treated in the previous section, are only an idealization which may be applied to rapid insertions in thermal reactors. More realistic simulations of superprompt-critical reactivity insertions, especially in the case of fast reactors, must account for the reactivity insertion rate (ramp rate) and the rapid flux response that occurs *during* and not *after* a reactivity insertion as in the case of step approximation. In the theoretical treatment, the ramp is unterminated, whereas in real situations the ramps are always terminated at some maximum available reactivity. Again, as in the previous case of step insertion, it is desirable to investigate the parametric dependencies of power and energy release on ramp rate, prompt-neutron generation time and reactivity coefficient.

The starting point is the prompt kinetics approximation, Eqs. (31) and (32), with the step reactivity replaced by a ramp insertion according to Eq. (11). It is convenient to begin the time scale at the instant when superprompt criticality is attained. The prompt-critical reactivity is then given by

$$\rho_p(t) = \dot{\rho}t - |\gamma| \int_0^t (p(t') - p_0)\, dt' \tag{39}$$

where the adiabatic condition with the stationary cooling, described by the term " $-p_0$" in the integrand of Eq. (39), is now included in the feedback reactivity since it modifies only the ramp rate

$$\dot{\rho}' = \dot{\rho} + |\gamma| p_0. \tag{40}$$

In the case of step-induced transients, stationary cooling was neglected for mathematical simplification. The Eqs. (32) and (39) are solved with the initial conditions

$$\rho_p(0) = 0$$

and the pseudo-initial power amplitude [1]

$$p(0) = p^0 \simeq p_0 \beta \left(\frac{2\pi}{\Lambda \dot{\rho}} \right)^{1/2}. \tag{41}$$

This system leads to a nonlinear differential equation which has been treated by several authors [7,8].

14

Initial results about essential characteristics of the transient are deduced directly from the differential equation as it was done for step-induced transients. More details are given in *Appendix 3*. It follows from Eq. (32) that $\dot{p}(t)$ and $\rho_p(t)$ pass through zero simultaneously, i.e.

$$\dot{p}(t) = 0, \quad \text{when} \quad \rho_p(t) = 0.$$

The extrema of power coincide with the zeros of reactivity:

$$\rho_p(t) = 0 \quad \text{and} \quad p(t) = \begin{Bmatrix} p_{max} \\ p_{min} \end{Bmatrix} \quad \text{at} \quad t = \begin{Bmatrix} t_{max} \\ t_{min} \end{Bmatrix}. \tag{42}$$

Additional information is obtained by investigating the extrema of $\rho_p(t)$, which occur at $t = t^{max}$ and $t = t^{min}$. Setting the time derivative of Eq. (39) to zero gives

$$\dot{\rho}_p(t) = \dot{\rho}' - |\gamma|\, p(t) = 0,$$

or

$$p(t) = \frac{\dot{\rho}'}{|\gamma|} = \bar{p} \quad \text{at} \quad t = \begin{Bmatrix} t^{max} \\ t^{min} \end{Bmatrix} \tag{43}$$

where $\bar{p}$ is the average power during the burst (see *Appendix 3*). From this equation it follows that the power amplitude at the extrema of the reactivity is equal to the average power $\bar{p}$, i.e. the extrema of the reactivity coincide with p(t) passing through $\bar{p}$. It has been demonstrated [7,8] that the pulse shape is symmetric around the peak power value , periodic and undamped in the absence of delayed neutrons. Eq. (43) shows that the average power $\bar{p}$ is independent of the generation time and the initial power; it is the same for all bursts under the condition of the feedback model. It is interesting to note that in the case of a step-induced supercritical transient, information on the energy release was obtained by investigating the transition of ρ_p through zero. For a ramp-induced transient, information on the average power is obtained instead. The difference occurs because only the rate of reactivity insertion is given for a ramp-induced transient, which then determines the rate of energy release, i.e. the power.

It is shown in *Appendix 3* that the criterion for the transition to the superprompt-critical domain is given by $\bar{p} \geq p^0$. Only then, the prompt kinetics model can be applied. The critical value of ramp rate which corresponds to this criterion is derived to (see Eq. (A.3.15)):

$$\dot{\rho}' = \left(|\gamma|\,\beta p_0 \right)^{\frac{2}{3}} \left(\frac{2\pi}{\Lambda} \right)^{\frac{1}{3}}. \tag{44}$$

The maximum value of superprompt-critical reactivity which can be inserted in a ramp is given by (see Eq. (A.3.14))

$$\rho_p^{max} = \sqrt{2\Lambda\dot{\rho}'\left[\ln\left(\frac{\bar{p}}{p^0} \right) - 1 + \frac{p^0}{\bar{p}} \right]}. \tag{45}$$

This value is attained when the power passes through $\bar{p}$. The reactivity then decreases until the minimum is attained with

$$\rho_p^{min} = -\rho_p^{max}.$$

Eq. (45) indicates that, in principle, high ramp rates can drive thermal systems to much higher superprompt-critical reactivities than fast systems due to the longer generation time.

Using reasonable physical approximations, it is possible to obtain estimates for the maximum power and total energy release without solving for $p(t)$ and $I(t)$. This is shown in *Appendix 3*. The results are given here. The power rise is

$$p_{max} - p^0 = \frac{\dot{\rho}'}{|\gamma|} \ln\left(\frac{p_{max}}{p^0}\right). \tag{46}$$

Assuming $p_{max} \gg p_0$ and neglecting the slowly varying logarithmic dependence, we have

$$p_{max} \propto \frac{\dot{\rho}'}{|\gamma|}. \tag{47}$$

The energy release in a burst is estimated to

$$I \simeq \frac{2}{|\gamma|} \sqrt{2\dot{\rho}'\Lambda\left[\ln\left(\frac{\bar{p}}{p^0}\right) - 1 + \frac{p^0}{\bar{p}}\right]}. \tag{48}$$

By using Eq. (45), this relation can be written as

$$|\gamma| I \simeq 2\rho_p^{max}.$$

It can then be interpreted as follows: the feedback corresponding to the energy released in a burst is twice the maximum inserted superprompt-critical reactivity. The feedback thus brings the reactivity from ρ_p^{max} to ρ_p^{min} from where the following pulse starts.

Neglecting the slowly varying logarithmic term in Eq. (48), we have

$$I \propto \frac{\sqrt{\dot{\rho}'\Lambda}}{|\gamma|}. \tag{49}$$

The burst width is proportional to I/p_{max}, or

$$\Gamma \propto \sqrt{\frac{\Lambda}{\dot{\rho}'}}. \tag{50}$$

From Eqs. (47), (49) and (50) it is obvious that the transients become more severe with increasing ramp rate and decreasing prompt negative feedback coefficient. In contrast to transients with step reactivity insertion, for ramp-induced transients the maximum power does not change when the prompt-neutron generation time is decreased, but energy release and pulse width both decrease.

The previous investigations are based on the prompt kinetics approximation with the linear energy model for the feedback reactivity, Eqs. (31) and (32). The delayed-neutron source is omitted. The effect of the delayed neutrons has been studied by several authors [1,7]. The results are as follows. During the first burst,

16

the prompt kinetics approximation yields fairly accurate results. The actual post-burst power is, however, higher if delayed neutrons are taken into account due to the source multiplication in a reactor close to prompt critical. This results in a substantial reactivity feedback even during the phase in which $p(t) < \bar{p}$. Therefore subsequent bursts are driven by a smaller effective reactivity ramp rate. A further contribution to the effect comes from an increase of the actual power at the start of the subsequent pulse: p^0 is bigger than in the preceding pulse and this reduces the peak power. As a consequence, the pulses are becoming asymmetrical and damped. The average power $\bar{p}$ remains constant as long as Eq. (31) is valid. It is the asymptotic value which is finally attained.

There is, however, a second effect which has not been taken into account in Eqs. (31) and (32). This is the temperature dependence of the prompt reactivity coefficient γ. According to Eq. (30), the contribution of the Doppler effect to the reactivity coefficient decreases with temperature. This has two effects: it increases the average power $\bar{p}$ and the peak power p_{max} as can be concluded from Eqs. (43) and (47). Since $\bar{p}$ increases with temperature, it follows that the power oscillates around a $\bar{p}$-curve that increases with time. These effects come out clearly from the Figs. 12 to 15 showing results obtained from calculations with the code DYANA2, which solves the set of simultaneous kinetics and thermal-hydraulics equations numerically, i.e. without making use of the prompt kinetics approximation.

III. Dynamics Calculations

In order to assess the validity of the different approximations and their range of applicability for rapid transients, calculations have been made with a dynamics code system which solves the complete set of kinetics and thermal-hydraulics equations including the delayed neutrons, temperature dependence of material properties and different feedback components. For these calculations, the dynamics code DYANA2, developed by SIEMENS (formerly INTERATOM), has been used [9]. The EFR design with a core height of 1 m has been adapted by SIEMENS to the DYANA2 code and data set together with code system were made available for use on the computer system at KfK [10].

III.1. The Dynamics Code System DYANA2

The dynamics code system DYANA2 has great flexibility due to its modular structure. It contains separate modules for network fluid dynamics and component thermal hydraulics and allows thus the simulation of different design features with a choice of model sophistication.

Important for our application is the modellization of the core and the consideration of different feedback reactivity contributions. The core is subdivided into a given number of parallel channels. Usually, a channel is used to represent an average pin in a fuel subassembly or a group of subassemblies. A channel can also be used to represent a blanket assembly or a control rod channel, and the hottest pin in a subassembly can be represented for safety analyses. Different channels can be used to account for radial and azimuthal power variations within the core, as well as variations in coolant flow and fuel burn-up. A channel includes the whole length of the subassembly, from coolant inlet to coolant outlet. Different

axial zones represent subassembly sections (fuel and axial blankets, gas plenum, upper and lower reflectors etc.).

The pin section is treated in more detail than the other sections. Each axial level contains radial nodes for fuel, coolant and structure (cladding and duct walls). Several radial nodes can be used in the fuel region to describe porosity distribution and restructured zones with fuel properties depending on temperature. The dependence of gap conductance on fuel and cladding temperature is described by using a formula that was calibrated with a fuel performance code. The model allows fuel melting between a solidus and liquidus point. Coolant boiling, however is not modelled. Reactivity includes contributions from the control and safety systems and feedback. The feedback reactivity contains local contributions from Doppler, fuel expansion, sodium and steel density as well as global contributions from radial core expansion, bowing and reactivity from control rod drive line expansion.

Fission power is calculated by point kinetics including delayed neutrons. Decay heat power can be chosen for each core channel and total power is liberated within the fuel. The simulation of primary and secondary systems as well as heat exchangers, pumps and plena is done in the EFR data set, but it is not important for our investigation because of the longer time constants involved.

III.2. Reactor Data and Conditions for Calculations

The EFR core is represented by seven channels which include three fuel regions at different burn-up stages, breeder and reflector assemblies, an internal storage and a hot channel for safety analyses. The major characteristics of the channels are summarized in Tab. 1, kinetic parameters are shown in Tab. 2. The temperature-dependent specific heat of the fuel is

$$c_f(T) = 0.2429 + 0.1854.10^{-3}T - 0.1599.10^{-6}T^2 + 0.5662.10^{-10}T^3$$

where $c_f(T)$ is in units of $(Jg^{-1}K^{-1})$ and T in (K). Fig. 4 shows a plot of c_f. It can be seen that the assumption of temperature-independence is only a very rough approximation.

Reactivity is inserted in the form of a ramp where the ramp rate is varied between a very slow value of 0.1 $/s to a very rapid value of 100 $/s. As soon as the ramp reaches a value of 3 $, the ramp is terminated and the reactivity remains constant for the rest of the calculation. In order to study the influence of prompt-neutron generation time on the results, its value, which is $\Lambda = 0.4x10^{-6}$ s for the EFR driver core, has been artificially modified.

Nominal power of the EFR driver core is 3600 MW$_{th}$. Its distribution to different channels is given in Tab. 1. The peak fuel temperature at nominal power is $T_{f,c} = 2200°C$. This value is attained in the hot channel with a peak linear heat rating of 410 W/cm at the central fuel node. A transient power rise would lead to early fuel melting. To avoid inconsistencies in the calculations due to the melting process, the initial power was decreased for this study to 20% of its nominal value. The peak fuel temperature is then $T_{f,c} = 820°C$ and there is a large range for fuel temperature rise before melting starts.

18

Channel no.	1	2	3	4	5	6	7
Group of S/As	Fuel 500 d BU	Fuel 1000 d BU	Fuel 1420 d BU	Breeder	Internal Storage	Reflectors, Shielding, Leakage	Fuel, max. loaded
Number of S/As	126	126	124	78	78	188	-
Number of Pins per S/A	331	331	331	169	331	19	331
S/A Flow (kg/s)	45.8	45.8	45.4	15.7	3.26	1.49	48.9
Total Flow (kg/s)	5774	5774	5635	1223	254	280	-
S/A Power (MW)	9.95	9.00	8.77	1.42	0.02	0.06	12.16
Temperature Rise (K)	171.4	155.0	152.3	71.6	5.3	31.8	196.0
Max. Linear Rating (W/cm)	336	304	298	94	0.7	35	410

Table 1. Core representation in DYANA2: Group of channels with power and flow distribution

Group of delayed neutrons i	λ_i [s^{-1}]	β_i
1	0.012966	0.72965×10^{-4}
2	0.031226	0.77734×10^{-3}
3	0.13433	0.61286×10^{-3}
4	0.34611	0.12273×10^{-2}
5	1.4038	0.56716×10^{-3}
6	3.7957	0.16012×10^{-3}

$$\beta = 341.77 \times 10^{-5}$$

$$\Lambda = 0.3886 \times 10^{-6} \text{ s}$$

Table 2. Kinetic parameters of the EFR core: Delayed neutron parameters

III.3. Results of Calculations and Discussion

Figs. 7 to 15 show power and net reactivity as a function of time for different values of prompt-neutron generation time and ramp rate. Regarding the time dependence of the net reactivity, we can clearly distinguish two different domains. The first is determined by the applied ramp and negligible feedback; the second is dominated by the feedback. The resulting power traces depend on the value of reactivity in the second domain: whether it remains subprompt critical or whether it enters into superprompt criticality. In the latter case, the transient is characterized by the occurrence of one or a series of pulses, i.e. an oscillation. For a part of the transients, the typical features of the power trace can be qualitatively derived on the basis of the Figs. 2 and 3.

In the first domain, determined by a constant ramp rate, the values of α are increasing according to the curves in Figs. 2 and 3, calculated for constant ramp rates. For slow ramps with $\dot{\rho} \leq 0.1$ $/s the α-values and thus the power shapes are independent of prompt-neutron generation time as long as the reactivity is not too close to prompt critical ($\rho \lesssim 0.9$ $). These conditions are met in Fig. 7 and the traces for different values of prompt-neutron generation time coincide. If the ramp rate is increased, slow systems are approaching the upper boundary for α-values, determined by Eq. (13) and indicated in Fig. 2, and their power rise will lag behind those of fast systems. This is the more so, the higher the ramp rate and the longer the prompt-neutron generation time. Slow systems cannot rise as rapidly as fast systems in case of faster ramp rates. This can be clearly seen in the initial phase of the power traces in Figs. 9 to 15.

As for the second domain, dominated by the feedback, we have to distinguish between transients where the reactivity remains always subprompt critical, and transients where the reactivity becomes superprompt critical. The first type will be considered first.

III.3.1. Subprompt-critical Transients

The initial power rise increases the feedback until it compensates the reactivity addition due to the ramp. With moderate ramp rates, this happens already before prompt criticality can be attained. The effective reactivity ramp being almost zero, the value of α is determined by the Nordheim relation (Eq. (14)). This results in nearly constant values of α which are then, however, smaller than during the initial phase. In this domain, the power is characterized by a nearly exponential growth. It can be seen from Fig. 1 that in cases of negligible ramp rate (0 $/s) the value of α is independent of the generation time as long as the generation time is not too long ($\Lambda \lesssim 10^{-4}$ s) and the reactivity is not too close to prompt critical ($\rho \lesssim 0.9$ $). We are then dealing with superdelayed-critical transients. In this situation, the transients are predominantly determined by the yields and half-lives of the delayed neutrons and the prompt-neutron generation time has thus no influence. Therefore, all power traces in Figs. 7 and 8 nearly coincide and display the typical shape of a superdelayed-critical transient which is characterized by an initial power rise entering into an exponential growth, terminated by the end of the ramp.

In Fig. 9 the initiation of an oscillation can be observed in the case of the slow system with $\Lambda = 10^{-4}$ s. The lag during the initial power rise leads to a later and

20

higher reactivity peak resulting in an overshoot and a subsequent undershoot compared with the other curves. The reactivity is, however, still subprompt-critical. The transients do not yet develop a burst structure and the power rise is still terminated by the end of the ramp insertion.

III.3.2. Superprompt-critical Transients

This picture changes if the ramp rate is further increased and the transients are entering into the superprompt-critical domain. The critical value when this occurs is given by Eq. (44). Fig. 16 shows the critical ramp rate as a function of generation time for different values of $|\gamma|$ and an initial power amplitude of $p_0 = 0.2$ fp. The upper value of $|\gamma|$ is representative for a fast reactors like EFR (see Fig.6) For thermal reactors, the lower values are more appropriate. In our calculations, however, the fast reactor values are used independent of the prompt-neutron generation time of the system. The slowest system with a generation time of 10^{-4} s becomes prompt critical slightly above a ramp rate of 1 \$/s. At 3 \$/s, the systems with 10^{-4} and 10^{-5} s both are superprompt-critical (see Fig. 10). The system with $\Lambda = 10^{-6}$ s becomes prompt critical at about 5 \$/s and EFR with $\Lambda = 0.4x10^{-6}$ s at about 7 \$/s. With a ramp rate of 6 \$/s, as shown in Fig. 11, EFR is still slightly subprompt critical. The curves in Fig. 16 indicate the regime of applicability of prompt kinetics; below these critical values it cannot be applied.

If a transient enters into the superprompt-critical domain, e.g. Fig. 10 for a ramp rate of 3 \$/s and $\Lambda = 10^{-4}$ s, the rapidly growing feedback brings the reactivity back to subprompt criticality, but the still continuing ramp leads back to the superprompt-critical domain inciting an oscillation. The oscillation is only cut off by the end of the ramp insertion. The system with $\Lambda = 10^{-5}$ s shows a short and small overshoot into superprompt criticality which damps out, however, very rapidly due to the effect of the delayed neutrons. Only the case with $\Lambda = 10^{-6}$ s remains subprompt-critical and shows still the typical features of a superdelayed-critical transient.

By further increasing the ramp rate to 10 \$/s (Fig. 12) all three transients have become superprompt-critical. The fast increase of α by passing from subprompt to superprompt criticality, as derived from Fig. 3, results in rapid power rises followed by rapid decreases after the peak. This is the typical superprompt-critical pulse shape or burst. As Eq. (45) shows, a short prompt-neutron generation time is advantageous in terminating the reactivity rise at an earlier stage. Fig. 17 shows the maximum superprompt-critical reactivity ρ_p^{max} as a function of prompt-neutron generation time. It is evident, that even rapid ramp rates can drive the reactivity of a fast system by only a fraction of a dollar beyond prompt critical. Much higher values are obtained, in principle, in thermal systems due to the larger prompt-neutron generation time.

The pulse width increases with the generation time as predicted by Eq. (50). Thermal systems are characterized by broad pulses. If the ramp rate is fast enough, the insertion time becomes shorter than the pulse width. In extreme cases, such as shown in Figs. 13 to 15 for the system with $\Lambda = 10^{-4}$ s, practically the total reactivity is inserted before any feedback has developed. We further observe that in this case energy release, pulse height and pulse width have become independent of the ramp rate. The Eqs. (47), (49) and (50) cannot be applied

for thermal systems in this regime of ramp rates and it is more appropriate to apply the model of step insertion of reactivity (see Section II.6.1).

With the knowledge of prompt kinetics, it is possible to assess the threshold value of ramp rate beyond which the conditions of step insertion are met:

$$\rho_p^{max} \gtrsim \rho_p^{ex}$$

where ρ_p^{max} is the value calculated by using Eq. (45) and ρ_p^{ex} is the total prompt excess reactvity which is inserted by the ramp. In the case of step insertion we have $\rho_p^{ex} = \rho_0 - \beta$. In our calculations, this value is always 2 \$. The ramp rates for which these conditions are met, can be obtained from Fig. 17. With $\rho_p^{ex}= 2$ \$, the values are 20 \$/s for a system with 10^{-4} s, 130 \$/s for a system with 10^{-5} s and 1000 \$/s for a system with 10^{-6} s.

The model of step insertion predicts, according to Eq. (37), an energy release taking place in a single pulse with a value independent of generation time. Thermal systems have broad pulses and small peaks (Eqs. (38) and (36)), fast systems, however, short pulses with high peaks. This can be seen by comparison of the pulse shapes of the systems with 10^{-4} s and 10^{-5} s in Figs. 14 and 15. The transient with 10^{-5} s is approaching a peak power of $p_{max} \simeq 2000$ fp which is about 10 times the value of the system with 10^{-4} s. This confirms the $\frac{1}{\Lambda}$ - dependence of p_{max} predicted by Eq. (36).

After having discussed the superdelayed-critical domain for slow ramp rates and the single pulse domain for very fast ramp rates, we will now turn our attention to the intermediate range. As soon as the ramp rate exceeds the critical value defined by Eq. (44), the reactivity passes into the superprompt-critical domain which is characterized by the appearance of power bursts. This is the regime where the prompt kinetics model can be applied. The number of pulses which appear depends on special conditions.

If the reactivity is approaching prompt criticality, the value of α changes rapidly. In the case of a fast system the increase is 2 to 3 orders of magnitude between 0.9 and 1.1 \$ (see Fig. 1) The prompt kinetics model predicts the appearance of periodic pulses. The pulse width is determined, according to Eq. (50), by the ratio of prompt-neutron generation time and ramp rate. Fast systems have short pulses and high frequency and slow systems have broad pulses and low frequency. The number of oscillations is limited by the duration of the ramp insertion. For a given ramp rate, the number of pulses increases if the prompt-neutron generation time decreases.

In a real system with consideration of delayed neutrons, the oscillations are damped or even suppressed if the reactivity becomes only slightly superprompt critical. The peak power values in fully developed oscillations are almost independent of prompt-neutron generation time and increase with the ramp rate according to Eq. (47). The energy release in a burst is increasing with prompt-neutron generation time and ramp rate. We observe therefore a number of small releases in fast systems instead of a big one in a thermal system (see Fig. 19).

Power oscillations are only possible between the values of transition to prompt critical and to the single-pulse regime shown in Fig. 18. The upper limit is determined by the duration of the reactivity ramp. If ρ_p^{max}, according to Eq. (45), is only

22

a small fraction of a dollar, a second transition to the superprompt-critical domain is suppressed due to the effect of the delayed neutrons. A short generation time is advantageous to meet this condition. The occurrence of more than one burst, i.e. a power oscillation, is possible, if the duration of the ramp is a few times the pulse width. For thermal systems this condition is only met within a small range of ramp rates. For fast systems this range is broader. The different regimes of transients are indicated in Fig. 18.

IV. Conclusions

Ramp-induced transients develop different types of power traces depending on ramp rate and prompt-neutron generation time. If the ramp rate is very slow, e.g. $\dot{\rho} < 0.1 \, \$/s$, the reactivity is compensated by feedback and the reactor passes through a sequence of near-equilibrium conditions.

With increasing ramp rate the feedback can no longer respond fast enough to compensate for the reactivity insertion and the properties of delayed neutrons become important determining the neutron kinetics of the transient, independent of prompt-neutron generation time. The reactivity remains, however, subprompt critical.

If reactivity is added so fast that the net reactivity rises above prompt critical before feedback becomes effective, power bursts develop and, if the duration of ramp insertion is long enough, power oscillations occur. In this regime, the prompt kinetics can be applied. Ramp rate and prompt-neutron generation time have a strong influence on energy release in a pulse and pulse width, the peak power, however, depends only on the ramp rate.

In the extreme case, where reactivity insertion is completed before feedback effects are effective in reducing the inserted reactivity, a single-pulse transient appears, the energy of which is independent of ramp rate and prompt-neutron generation time. It depends only on the magnitude of the reactivity. In this regime the model of step-insertion is applicable.

In order to compare transients in systems with different values of prompt-neutron generation time, i.e. fast reactors with light water- or graphite-moderated reactors, the ramp rate has to be determined. Which model is applicable in a given case, depends on the transient regime defined by ramp rate and prompt-neutron generation time. The influence of delayed neutrons as well as the temperature dependence of the prompt energy coefficient of reactivity complicate the situation and restrict the applicability of simple models. However, they can be useful for qualitative discussion and physical understanding of the phenomena.

References

[1] K.E.Ott and R.J.Neuhold, "Nuclear Reactor Dynamics", La Grange Park, Illinois (1985).

[2] G.R.Keepin, "Physics of Nuclear Kinetics", Addison-Weseley, Reading, Mass. (1965).

[3] E.E.Lewis, "Nuclear Power Reactor Safety", J.Wiley & Sons, New York (1977).

[4] D.Smidt, "Reaktortechnik", Bd.2, G.Braun, Karlsruhe (1971).

[5] A.E.Waltar and A.B.Reynolds, "Fast Breeder Reactors", Pergamon Press, New York (1981).

[6] G.Kussmaul et al., "Startup Measurements on the CABRI Reactor", *Proc. Int. Meeting on Fast Reactor Safety Technologies*, Seattle, 1979, Vol.V, p.2322.

[7] W.Häfele, "Prompt überkritische Leistungsexkursionen in schnellen Reaktoren", *Nukleonik* **5**, p.201 (1963).

[8] R.Fröhlich and S.R.Johnson, "Exact Solution of the Non-linear Prompt Kinetics Equations - A Benchmark Problem in Reactor Kinetics", *Nukleonik* **12**, p.93 (1969).

[9] V.Ertel and R.Reinders, "Development and Application of the Thermohydraulic System Code DYANA/ATTICA", *Proc. Int. Conf. Science and Technology of Fast Reactor Safety*, St. Peter Port, Guernsey, 1986, Vol.2, p.191.

[10] V.Ertel, SIEMENS, pers. communication (1992).

Appendix 1: Instantaneous Reciprocal Period

Eq. (10) can be obtained from Eqs. (5) and (6) by first dividing Eq. (5) by p(t) and then eliminating p(t) in the second right-side term by using the Eqs. (6). This leads to the expression

$$\alpha(t) = \frac{\rho(t) - \beta}{\Lambda} + \frac{\beta}{\Lambda} \sum_{i=1}^{N} \frac{a_i \lambda_i}{\lambda_i + \dot{c}_i/c_i}$$

which can be rearranged by using the identity

$$\sum_{i=1}^{N} \frac{a_i \lambda_i}{\lambda_i + \dfrac{\dot{c}_i}{c_i}} = 1 - \sum_{i=1}^{N} \frac{a_i}{1 + \dfrac{\lambda_i}{\dot{c}_i/c_i}}$$

to give finally the expression of Eq. (10).

Appendix 2: Step Insertions

We start with Eq. (32)

$$\dot{p}(t) = \frac{\rho_p(t)}{\Lambda} p(t) \qquad (A.2.1)$$

where

$$\rho_p(t) = \rho_0 - \beta - |\gamma| \int_0^t p(t')dt' \qquad (A.2.2)$$

and $\rho_0 > \beta$ is the step reactivity inserted at $t = 0$. The initial values are given by

$$\rho_p(0) = \rho_0 - \beta \quad \text{and} \quad \dot{\rho}_p(0) = -|\gamma|p^0. \qquad (A.2.3)$$

Eq. (A.2.2) can be differentiated twice to give

$$\dot{\rho}_p(t) = -|\gamma| \, p(t) \qquad (A.2.4)$$

and

$$\ddot{\rho}_p(t) = -|\gamma| \, \dot{p}(t). \qquad (A.2.5)$$

By combination of Eq. (A.2.5) with (A.2.1) and (A.2.4) we obtain

$$\Lambda \ddot{\rho}_p(t) = \rho_p(t) \, a_p(t). \qquad (A.2.6)$$

This nonlinear second-order differential equation can be solved by integration:

$$\Lambda \int_0^t \frac{d\dot{\rho}_p}{dt'} \, dt' = \int_0^t \rho_p(t) \, \frac{d\rho_p}{dt'} \, dt'$$

which gives the first integral in the form

$$\Lambda \left[\dot{\rho}_p(t) - \dot{\rho}_p(0) \right] = \frac{1}{2} \left[\rho_p{}^2(t) - \rho_p{}^2(0) \right]. \qquad (A.2.7)$$

Inserting the initial values and Eq. (A.2.4) results in the following form of the first integral:

$$\Lambda \, |\gamma| \left[p^0 - p(t) \right] = \frac{1}{2} \left[\rho_p{}^2(t) - (\rho_0 - \beta)^2 \right]. \qquad (A.2.8)$$

This integral is investigated at the time of the power maximum, $t = t_{max}$, where $\rho_p(t) = 0$ and $p(t) = p_{max}$. This gives

$$p_{max} - p^0 = \frac{(\rho_0 - \beta)^2}{2\Lambda|\gamma|}. \qquad (A.2.9)$$

The power rise, $p_{max} - p_0$, is independent of the initial power.

The first integral, Eq. (A.2.8), also provides information on the total reactivity feedback during the the transient. If we consider the transient terminated, when

$p(t)$ has returned to the initial value, p^0, say at $t = t_2$, the left side of Eq. (A.2.8) vanishes and thus

$$\rho_p^2(t) = (\rho_0 - \beta)^2 \quad \text{for} \quad t = 0 \quad \text{and} \quad t_2$$

with the two solutions

$$\rho_p(0) = (\rho_0 - \beta) \quad \text{at} \quad t = 0$$

and

$$\rho_p(t_2) = -(\rho_0 - \beta) \quad \text{at} \quad t = t_2. \tag{A.2.10}$$

The prompt feedback compensates the prompt reactivity twice during during the transient or the reactivity swing is just two times the initial prompt reactivity.

If we insert the last value into Eq. (A.2.2) we can derive a value for the total energy release during the transient:

$$I(t_2) \equiv \int_0^{t_2} p(t')dt' = 2\frac{(\rho_0 - \beta)}{|\gamma|}. \tag{A.2.11}$$

The total energy release during a superprompt-critical transient is independent of the prompt-neutron generation time Λ, as it is for delayed supercritical transients.

The first integral in the form of Eq. (A.2.7) is a first-order differential equation for $\rho_p(t)$ that may be solved readily. Then $p(t)$ can be derived from $\rho_p(t)$ using Eq. (A.2.4). Rearranging the first integral, Eq. (A.2.7), using Eq. (A.2.3) yields

$$2\Lambda\dot{\rho}_p(t) = \rho_p^2(t) - \rho_b^2 \tag{A.2.12}$$

with

$$\rho_b^2 = \rho_p^2(0) + 2\Lambda|\gamma|p^0. \tag{A.2.13}$$

Dividing Eq. (A.2.12) by its right hand side and integrating with respect to time from 0 to t yields, after changing the integration limits and rearrangement,

$$t = 2\Lambda \int_{\rho_p(t)}^{\rho_p(0)} \frac{d\rho_p}{\rho_b^2 - \rho_p^2(t)} = \frac{2\Lambda}{\rho_b} \int_{\frac{\rho_p(t)}{\rho_b}}^{\frac{\rho_p(0)}{\rho_b}} \frac{d\left(\frac{\rho_p}{\rho_b}\right)}{1 - \left(\frac{\rho_p(t)}{\rho_b}\right)^2}.$$

The integration of the right hand side expression of this equation gives

$$t = \frac{2\Lambda}{\rho_b}\left[\tanh^{-1}\left(\frac{\rho_p(0)}{\rho_b}\right) - \tanh^{-1}\left(\frac{\rho_p(t)}{\rho_b}\right)\right]. \tag{A.2.14}$$

Since $\rho_p(t) = 0$ and $\tanh^{-1}(0) = 0$ at the time of the power peak, $t = t_{max}$, we obtain

$$t_{max} = \frac{2\Lambda}{\rho_b} \tanh^{-1}\left(\frac{\rho_p(0)}{\rho_b} \right).$$

Insertion into Eq. (A.2.14) gives the solution of the differential equation, Eq. (A.2.6):

$$-\frac{\rho_b}{2\Lambda}(t - t_{max}) = \tanh^{-1}\left(\frac{\rho_p(t)}{\rho_b} \right)$$

or in its inverted form

$$\rho_p(t) = \rho_b \tanh\left(-\frac{\rho_b}{2\Lambda}(t - t_{max}) \right). \qquad (A.2.15)$$

The result is the hyperbolic function $\tanh(\tau)$. By using its special properties, we can find some features of the reactivity $\rho_p(t)$. First, $\tanh(\tau)$ is an odd or antisymmetric function, i.e. $\tanh(\tau) = -\tanh(-\tau)$, furthermore $\tanh(\tau) > 0$ for $\tau > 0$ and finally $\tanh(0) = 0$. Thus we find

$$\rho(t) \begin{Bmatrix} > \\ = \\ < \end{Bmatrix} 0, \quad \text{for } t - t_{max} \begin{Bmatrix} < \\ = \\ > \end{Bmatrix} 0, \quad \text{or } t \begin{Bmatrix} < \\ = \\ > \end{Bmatrix} t_{max}.$$

$\rho_p(t)$ is antisymmetric around t_{max}. The prompt reactivity is reduced from its initial value at $t = 0$, i.e. $\rho_p(0)$, to zero at $t = t_{max}$ and and to $-\rho_p(0)$ at $t = 2t_{max}$. By comparison with Eq. (A.2.10) we find that $t_2 = 2t_{max}$. In order to derive the power, Eq. (A.2.4) can be used

$$p(t) = -\frac{\dot{\rho}_p(t)}{|\gamma|} = -\frac{\rho_b}{|\gamma|} \frac{d}{dt} \tanh\left(-\frac{\rho_b}{2\Lambda}(t - t_{max}) \right)$$

$$= -\frac{\rho_b}{|\gamma|} \frac{1}{\cosh^2\left(-\frac{\rho_b}{2\Lambda}(t - t_{max}) \right)} \left(-\frac{\rho_b}{2\Lambda} \right)$$

or with Eq. (A.2.9) inserted

$$p(t) = \frac{p_{max}}{\cosh^2\left(\frac{\rho_b}{2\Lambda}(t - t_{max}) \right)} \qquad (A.2.16)$$

where we have used the property of symmetry for $\cosh(-\tau) = \cosh(\tau)$ and the relation derived from Eqs. (A.2.13) and (A.2.9):

$$\frac{\rho_b^2}{2\Lambda|\gamma|} = \frac{\rho_p^2(0)}{2\Lambda|\gamma|} + p^0 = p_{max}. \qquad (A.2.17)$$

From the symmetry property of $\cosh(\tau)$ we derive that $p(t)$ is symmetrical around t_{max}. Therefore Eq. (A.2.11) can be replaced by

$$I(t = 2t_{max}) = 2\int_0^{t_{max}} p(t')dt' = 2\frac{(\rho_0 - \beta)}{|\gamma|}. \qquad (A.2.18)$$

The pulse width Γ is defined by

$$\Gamma = \frac{1}{P_{max}} \int_0^{2t_{max}} p(t)dt = \frac{2}{P_{max}} \frac{\rho_p(0)}{|\gamma|}$$

where the peak power value is given by Eq. (A.2.9). By using this equation and the identity

$$\frac{1}{P_{max}} \equiv \frac{1}{P_{max} - p^0}\left(1 - \frac{p^0}{P_{max}}\right)$$

we obtain

$$\Gamma = \frac{4\Lambda}{\rho_p(0)}\left(1 - \frac{p^0}{P_{max}}\right). \tag{A.2.19}$$

If $P_{max} \gg p^0$, the pulse width becomes

$$\Gamma \simeq \frac{4\Lambda}{\rho_p(0)} \tag{A.2.20}$$

or four times the initial period (see Eq. (A.2.1))

$$\left(\frac{1}{\alpha}\right)_0 = \lim_{t \to 0} \frac{p(t)}{\dot{p}(t)} = \frac{\Lambda}{\rho_p(0)}.$$

The proportionality of Γ to Λ compensates the $1/\Lambda$-dependence of p_{max} and thus yields a Λ-independent energy production.

Appendix 3: Ramp Insertions

The basis of the treatment of ramp reactivity insertions is Eq. (32):

$$\dot{p}(t) = \frac{\rho_p(t)}{\Lambda} p(t). \qquad (A.3.1)$$

It is assumed that the reactor becomes prompt critical at $t = 0$. Only then, the reactivity ramp is applied in Eq. (A.3.1). The reactivity for ramp insertions is

$$\rho_p(t) = \dot{\rho}t - |\gamma| \int_0^t (p(t') - p_0)\, dt'. \qquad (A.3.2)$$

The stationary cooling described by the term $"-p_0"$ in the integrand of Eq. (A.3.2) is now included in the feedback reactivity since it modifies only the ramp rate

$$\dot{\rho}' = \dot{\rho} + |\gamma| p_0.$$

In the case of step-induced transients, stationary cooling was neglected for mathematical simplification. Instead of Eq. (A.3.2), the reactivity is now written as

$$\rho_p(t) = \dot{\rho}'t - |\gamma| \int_0^t p(t')\, dt' \qquad (A.3.3)$$

and we obtain also its time derivative

$$\dot{\rho}_p(t) = \dot{\rho}' - |\gamma| p(t). \qquad (A.3.4)$$

The Eqs. (A.3.1) and (A.3.3) are solved with the initial conditions

$$\rho_p(0) = 0$$

and the pseudo-initial power amplitude [4].

$$p(0) = p^0 \simeq p_0 \beta \left(\frac{2\pi}{\Lambda \dot{\rho}} \right)^{1/2}. \qquad (A.3.5)$$

Initial results about essential characteristics of the transient can be deduced directly from the Eqs. (A.3.1), (A.3.3) and (A.3.4) as it was done for step-induced transients.

First we consider the points in time when $\rho_p(t)$ passes through zero. It follows from Eq. (A.3.1) that $\dot{p}(t)$ and $\rho_p(t)$ pass through zero simultaneously, i.e.

$$\dot{p}(t) = 0, \quad \text{when} \quad \rho_p(t) = 0.$$

Thus, the extrema of the power coincide with the zeros of the reactivity.

Since $\rho_p(t)$ is zero initially, p(t) starts with zero slope and has a minimum at $t = 0$. Subsequently, $\rho_p(t)$ and thus p(t) both increase. With increasing accumulation of energy, the reactivity feedback, i.e. the 2nd term in the right hand side of Eq. (A.3.3), increases until it overcomes the ramp reactivity and $\rho_p(t)$ is again reduced to zero, say at $t = t_{max}$. The power has a maximum at this time. The feedback in-

creases even during the power reduction and $\rho_p(t)$ becomes more and more negative. However, as the ramp continues to increase the reactivity, it overrides finally the negative reactivity resulting from the power pulse and passes again through zero at $t = t_{min}$. At this time, a second power minimum occurs and the reactor starts on a second power burst. It has been demonstrated that the pulse shape is symmetric around the peak power value, periodic and undamped in the absence of delayed neutrons [7,8].

Thus, for the first extremum of power, we find

$$\rho_p(t) = 0 \quad \text{and} \quad p(t) = \begin{Bmatrix} p_{max} \\ p_{min} \end{Bmatrix} \quad \text{at} \quad t = \begin{Bmatrix} t_{max} \\ t_{min} \end{Bmatrix}. \tag{A.3.6}$$

Additional information is obtained by investigating the extrema of $\rho_p(t)$, i.e. the points in time when $\dot{\rho}_p(t) = 0$. Setting the time derivative of Eq. (A.3.4) to zero gives

$$\dot{\rho}_p(t) = \dot{\rho}' - |\gamma|\, p(t) = 0$$

or

$$p(t) = \frac{\dot{\rho}'}{|\gamma|} \quad \text{at} \quad t = \begin{Bmatrix} t^{max} \\ t^{min} \end{Bmatrix}. \tag{A.3.7}$$

Since the minima of power occur when $\rho_p(t)$ passes through zero, a relation between the reactivity insertion and the feedback during a burst can be obtained from Eq. (A.3.3) by considering the integration between two successive zeros of $\rho_p(t)$:

$$\dot{\rho}'\, \Delta t - |\gamma| \int_{\Delta t} p(t')\, dt' = 0$$

or

$$\frac{\dot{\rho}'}{|\gamma|} = \frac{1}{\Delta t} \int_{\Delta t} p(t')\, dt' \equiv \bar{p} \tag{A.3.8}$$

where $\Delta t = t_{min}$ is the duration of the power burst and the right hand side of Eq. (A.3.8) is the "average" power during the burst, $\bar{p}$. Eq. (A.3.8) shows that the average power $\bar{p}$ is independent of the generation time and the initial power; it is the same for all bursts under the conditions of the feedback model. By comparison with Eq. (A.3.7) it follows that the power amplitude at the extrema of the reactivity is equal to the average power $\bar{p}$, i.e. the extrema of the reactivity coincide with p(t) passing through $\bar{p}$.

In order to solve Eqs. (A.3.1) and (A.3.3) with the initial conditions (Eq. (A.3.5)) we express Eq. (A.3.1) as

$$\frac{dp}{d\rho_p} \frac{d\rho_p}{dt} = \frac{\rho_p(t)}{\Lambda}\, p(t). \tag{A.3.9}$$

Insertion of Eq. (A.3.4) into Eq. (A.3.9) gives

$$\frac{dp}{p(t)} (\dot{p}' - |\gamma| p(t)) = \frac{\rho_p(t)}{\Lambda} d\rho_p. \qquad (A.3.10)$$

This nonlinear differential equation has been treated by several authors [4,7,8]. Eq. (A.3.10) may be integrated between t = 0 and t. Insertion of the initial conditions (Eq. (A.3.5)), yields $\rho_p(t)$ in terms of reactor power:

$$\frac{1}{2\Lambda} \rho_p^2(t) = \dot{p}' \ln\left(\frac{p(t)}{p^0}\right) - |\gamma| (p(t) - p^0). \qquad (A.3.11)$$

It is clear from the previous considerations which led to Eq. (A.3.6) that the maximum power, p_{max}, occurs when $\rho_p(t) = 0$. We thus have

$$p_{max} - p^0 = \frac{\dot{p}'}{|\gamma|} \ln\left(\frac{p_{max}}{p^0}\right). \qquad (A.3.12)$$

In contrast to step-induced transients, the power rise, $p_{max} - p^0$, does not depend on the prompt-neutron generation time Λ. It is, however, slightly dependent on the initial power. For estimates, the slowly varying logarithmic dependence can be neglected and we have in the case $p_{max} \gg p^0$

$$p_{max} \propto \frac{\dot{p}'}{|\gamma|}. \qquad (A.3.13)$$

Eq. (A.3.11) gives two values for the reactivity

$$\rho_p(t) = \pm \sqrt{2\Lambda\dot{p}' \left[\ln\left(\frac{p(t)}{p^0}\right) - \frac{|\gamma|}{\dot{p}'} (p(t) - p^0) \right]}.$$

The maximum and minimum of reactivity occur at $t = t^{max}$ and $t = t^{min}$, respectively, where $p(t) = \bar{p}$:

$$\rho_p^{max} = -\rho_p^{min} = \sqrt{2\Lambda\dot{p}' \left[\ln\left(\frac{\bar{p}}{p^0}\right) - 1 + \frac{p^0}{\bar{p}} \right]}. \qquad (A.3.14)$$

This equation shows that the reactivity maxima and minima are symmetric about $\rho_p = 0$ and that the values are increasing with $\dot{p}'$ and Λ. Values of ρ_p^{max} as a function of ramp rate are plotted in Fig. 17 for different values of prompt-neutron generation time.

Eq. (A.3.14) has real roots only if

$$\frac{\bar{p}}{p^0} \geq 1$$

where the value of $\bar{p}$ is given by Eq. (A.3.8) and of p^0 by Eq. (A.3.5). In the case $\bar{p} < p^0$, i.e. if Eq. (A.3.14) has no real roots, the prompt kinetics model cannot be applied. The inequality may be physically realized for small ramp rates and large feedback coefficients (small $\bar{p}$) or large pseudo-initial power values p^0. In such cases, the feedback effect during the subprompt-critical phase of the transient is

strong enough that the reactivity does not reach the superprompt-critical domain. The condition

$$\bar{p} = p^0$$

can therefore be used as a criterion for the transition to superprompt criticality. If we insert p^0 and $\bar{p}$ in Eqs. (A.3.5) and (A.3.8) we obtain after rearranging

$$\dot{\rho}' = \left(|\gamma|\beta p_0\right)^{\frac{2}{3}} \left(\frac{2\pi}{\Lambda}\right)^{\frac{1}{3}}. \tag{A.3.15}$$

Eq. (A.3.15) determines the critical ramp rate at which the transient enters into prompt criticality. Fig. 16 shows the critical ramp rate as a function of prompt-neutron generation time for the values $|\gamma| = 0.4$ \$/s and $p_0 = 0.2$ fp.

To obtain an estimate of the energy release in one pulse, we evaluate Eq. (A.3.3) at $t = t_{max}$, the time at which according to Eq. (A.3.6) $\rho_p(t) = 0$:

$$\int_0^{t_{max}} p(t)dt = \frac{\dot{p}t_{max}}{|\gamma|}. \tag{A.3.16}$$

Since the calculation of t_{max} is rather complicated, physical arguments are used to make two approximations. When the reactivity has passed its peak at $t = t^{max}$, the feedback increases rapidly and brings the the reactivity to zero at $t = t_{max}$. No great error is introduced in Eq. (A.3.16) by replacing t_{max} by t^{max}. Moreover, at $t = t^{max}$ there is very little reactivity feedback and we can replace the value of the ramp reactivity, $\dot{p}t^{max}$, by the actual value given by Eq. (A.3.14).

Finally, the energy release for the burst is estimated by assuming that the burst is symmetric about $t = t_{max}$, which gives an additional factor of 2:

$$I \simeq \frac{2}{|\gamma|} \sqrt{2\Lambda\dot{\rho}'\left[\ln\left(\frac{\bar{p}}{p^0}\right) - 1 + \frac{p^0}{\bar{p}}\right]}. \tag{A.3.17}$$

Neglecting the slowly varying logarithmic term, we have

$$I \propto \frac{\sqrt{\Lambda\dot{\rho}'}}{|\gamma|}. \tag{A.3.18}$$

The burst width is proportional to I/p_{max}, or

$$\Gamma \propto \sqrt{\frac{\Lambda}{\dot{\rho}'}}. \tag{A.3.19}$$

From Eqs. (A.3.13), (A.3.18) and (A.3.19), it is obvious that the transients become more severe with increasing ramp rate and decreasing prompt negative feedback coefficient. In contrast to step-induced transients, the maximum power does not change, when the prompt-neutron generation time Λ is decreased, the energy release, however, is decreased.
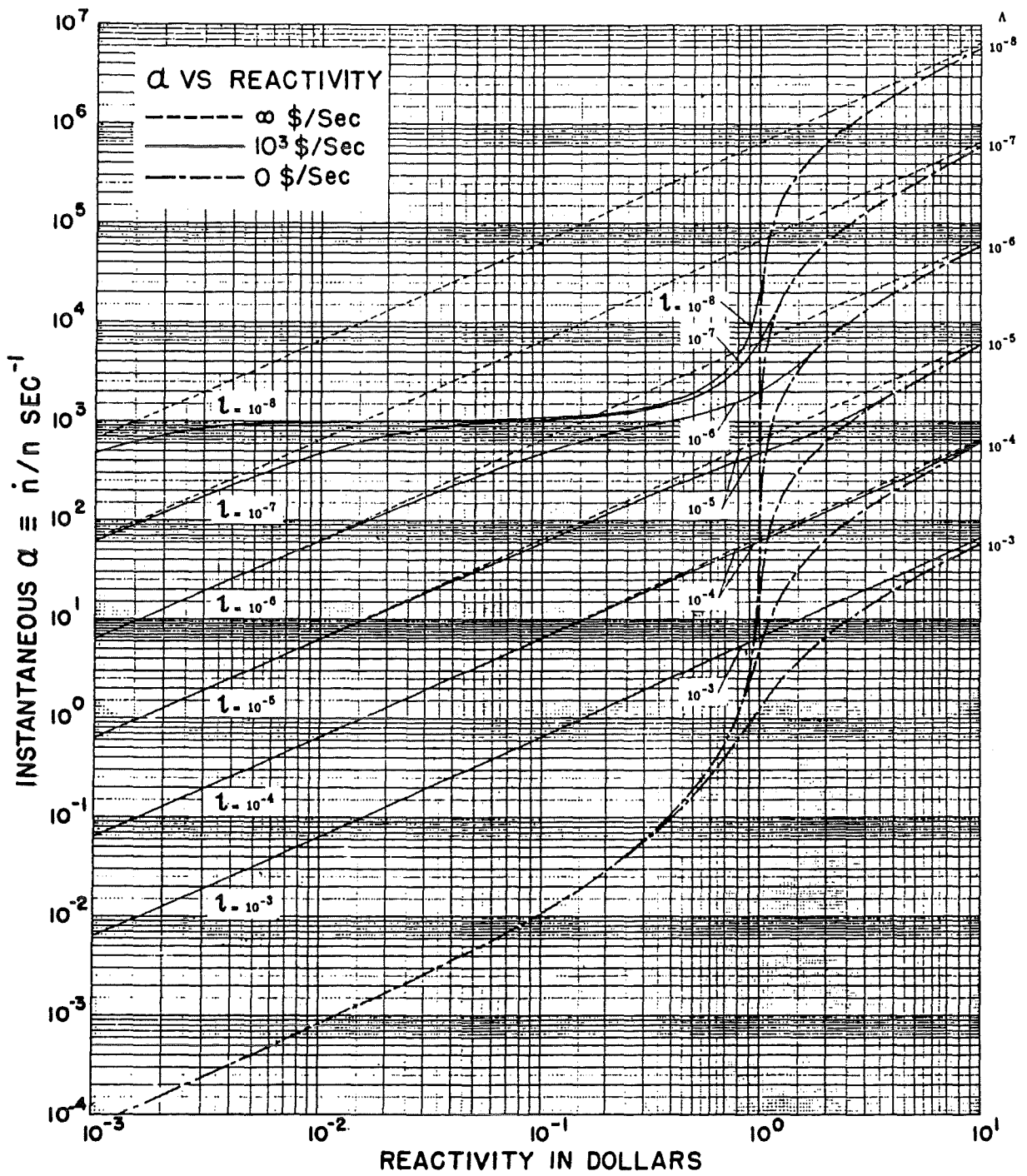
Figure 1. : Instantaneous α as a function of reactivity for U^{235}-systems with various prompt-neutron lifetimes and for ramp rates: 0 $/s, 1000 $/s, and ∞ $/s (from Ref. 2).

35
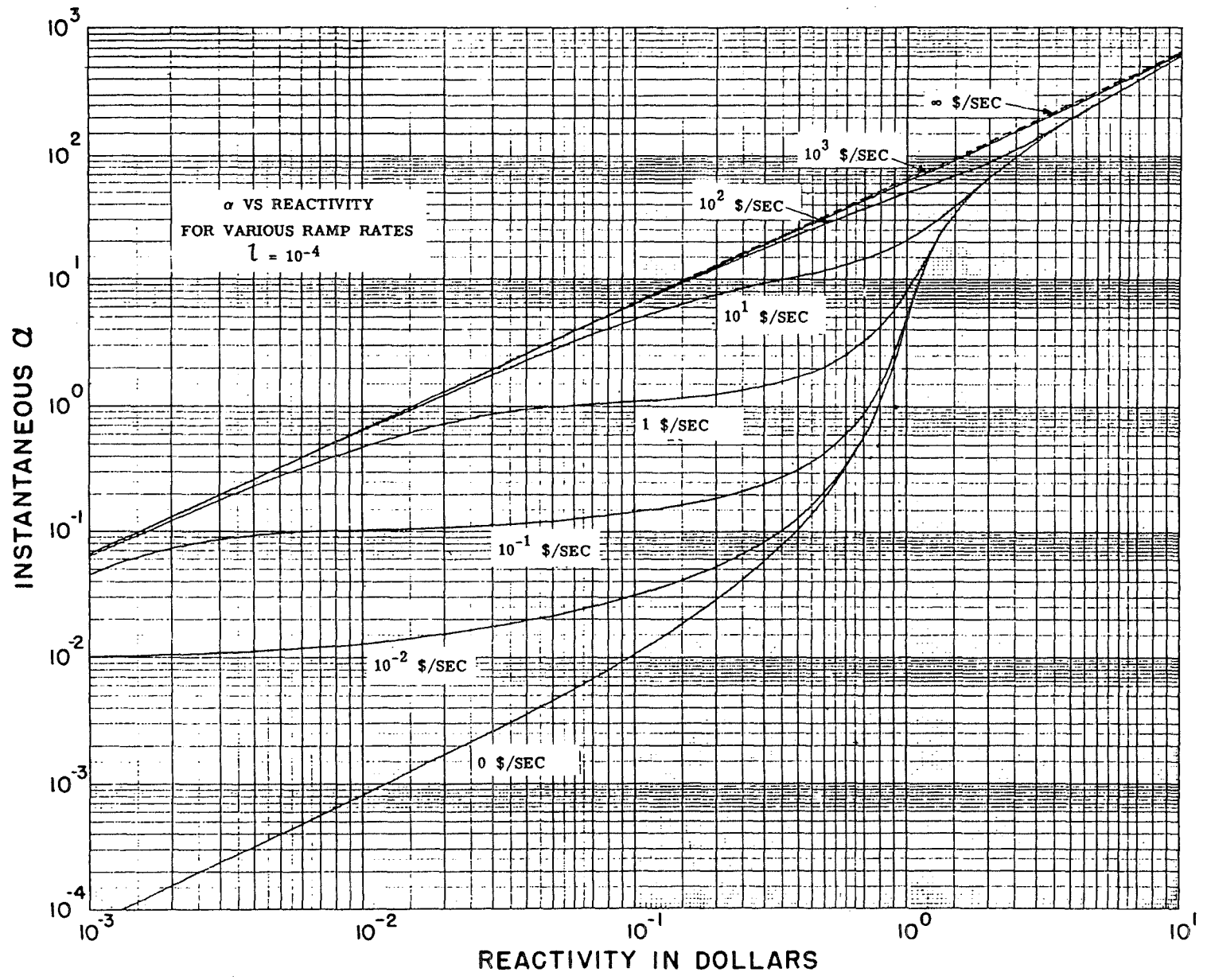
Figure 2. : Instantaneous α as a function of reactivity for various ramp rates. (U^{235}-system, prompt neutron lifetime = 10^{-4} s, from Ref. 2).
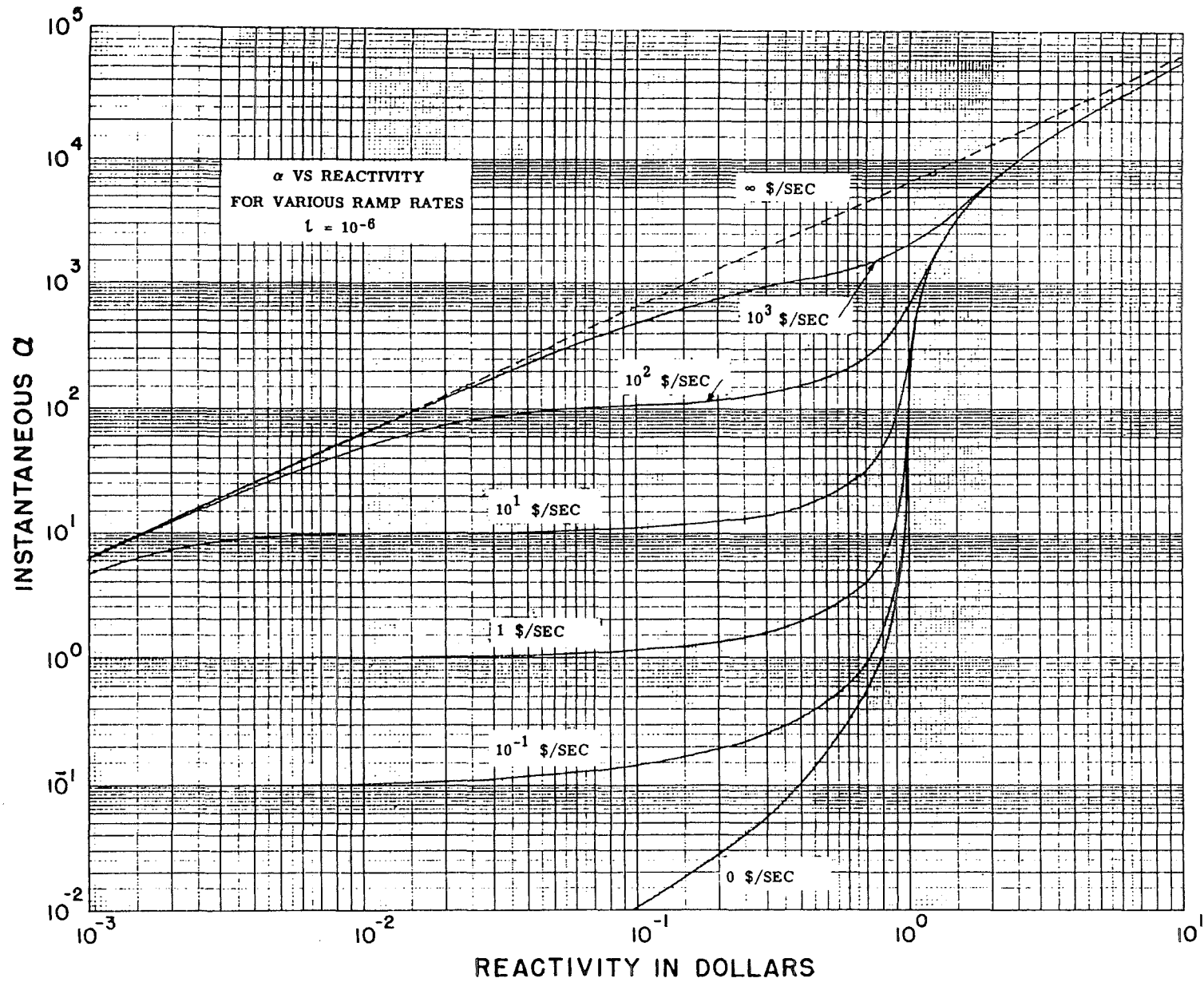
Figure 3. : Instantaneous α as a function of reactivity for various ramp rates. (U^{235}-system, prompt neutron lifetime $= 10^{-6}$ s, from Ref. 2).

The figure shows a graph with the following elements:

- Title box: α VS REACTIVITY FOR VARIOUS RAMP RATES, $l = 10^{-6}$
- Y-axis label: INSTANTANEOUS α, ranging from 10^{-2} to 10^5
- X-axis label: REACTIVITY IN DOLLARS, ranging from 10^{-3} to 10^1
- Curve labels: ∞ \$/SEC, 10^3 \$/SEC, 10^2 \$/SEC, 10^1 \$/SEC, 1 \$/SEC, 10^{-1} \$/SEC, 0 \$/SEC
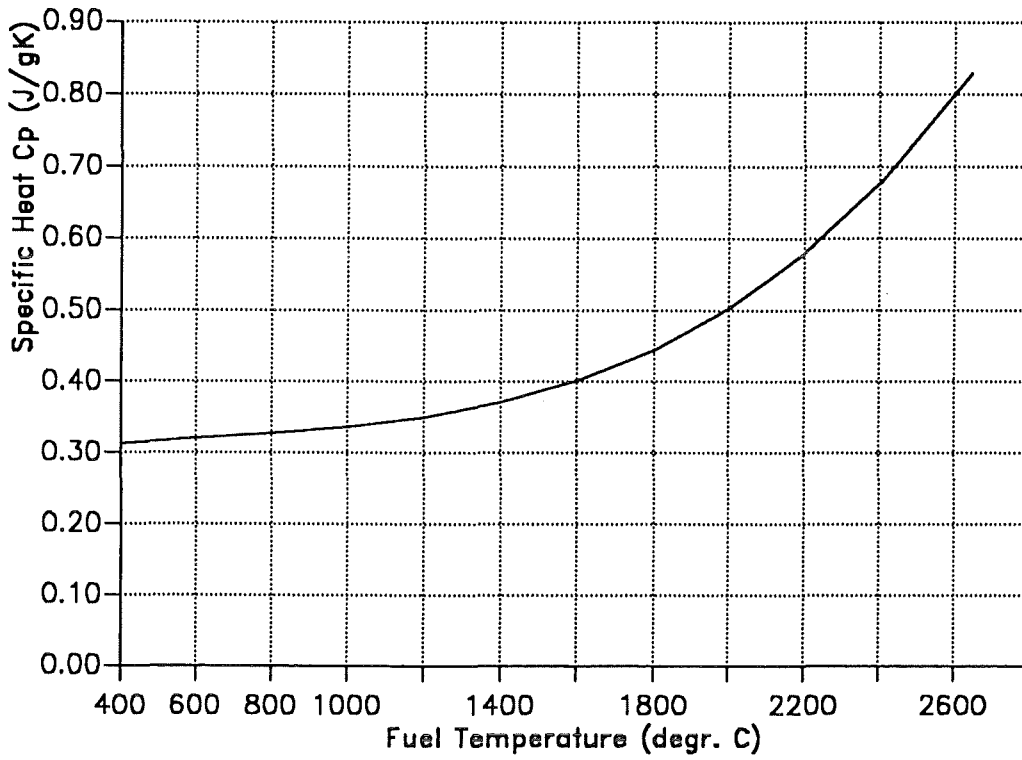
Figure 4. : Specific heat of EFR fuel used in DYANA2 calculations.
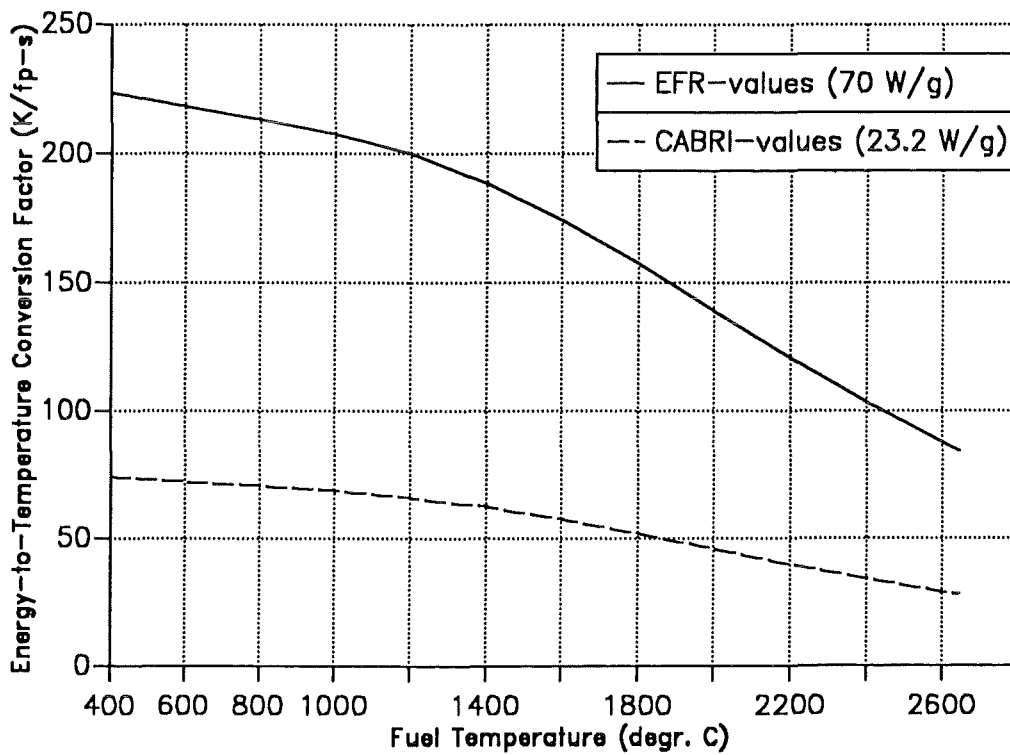
Figure 5. : Energy-to-temperature conversion factor for EFR and CABRI.
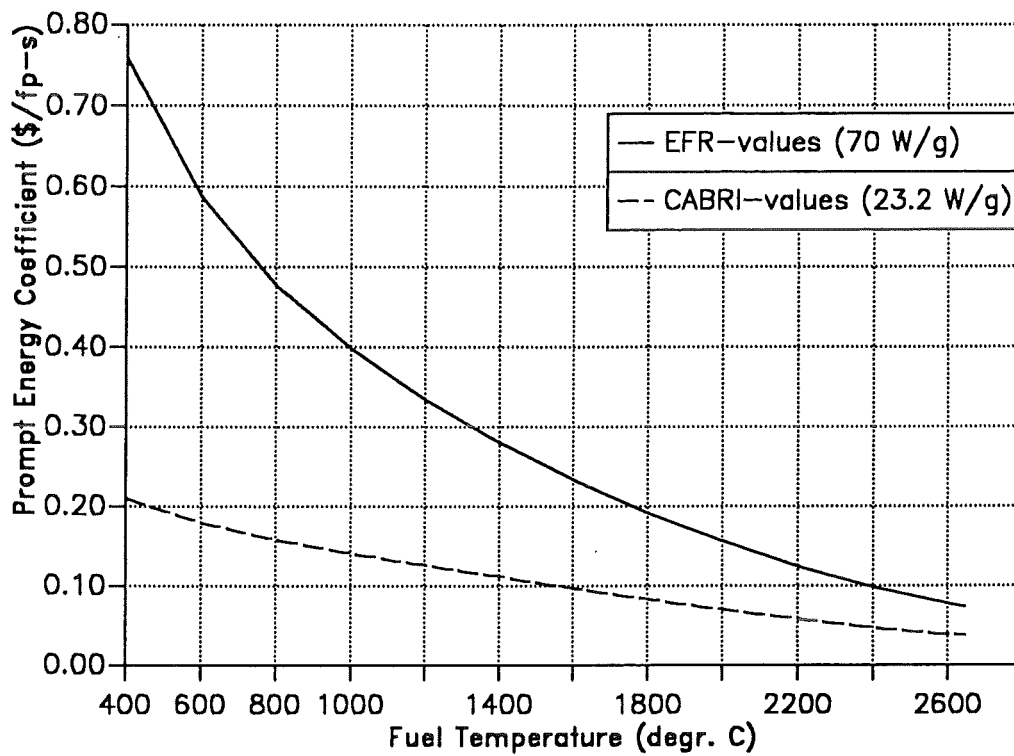
Figure 6. : Prompt energy coefficient for EFR and CABRI.

The figure shows a plot with axes:
- Y-axis: Prompt Energy Coefficient ($/fp-s) ranging from 0.00 to 0.80
- X-axis: Fuel Temperature (degr. C) ranging from 400 to 2600

Legend:
— EFR—values (70 W/g)
-- CABRI—values (23.2 W/g)
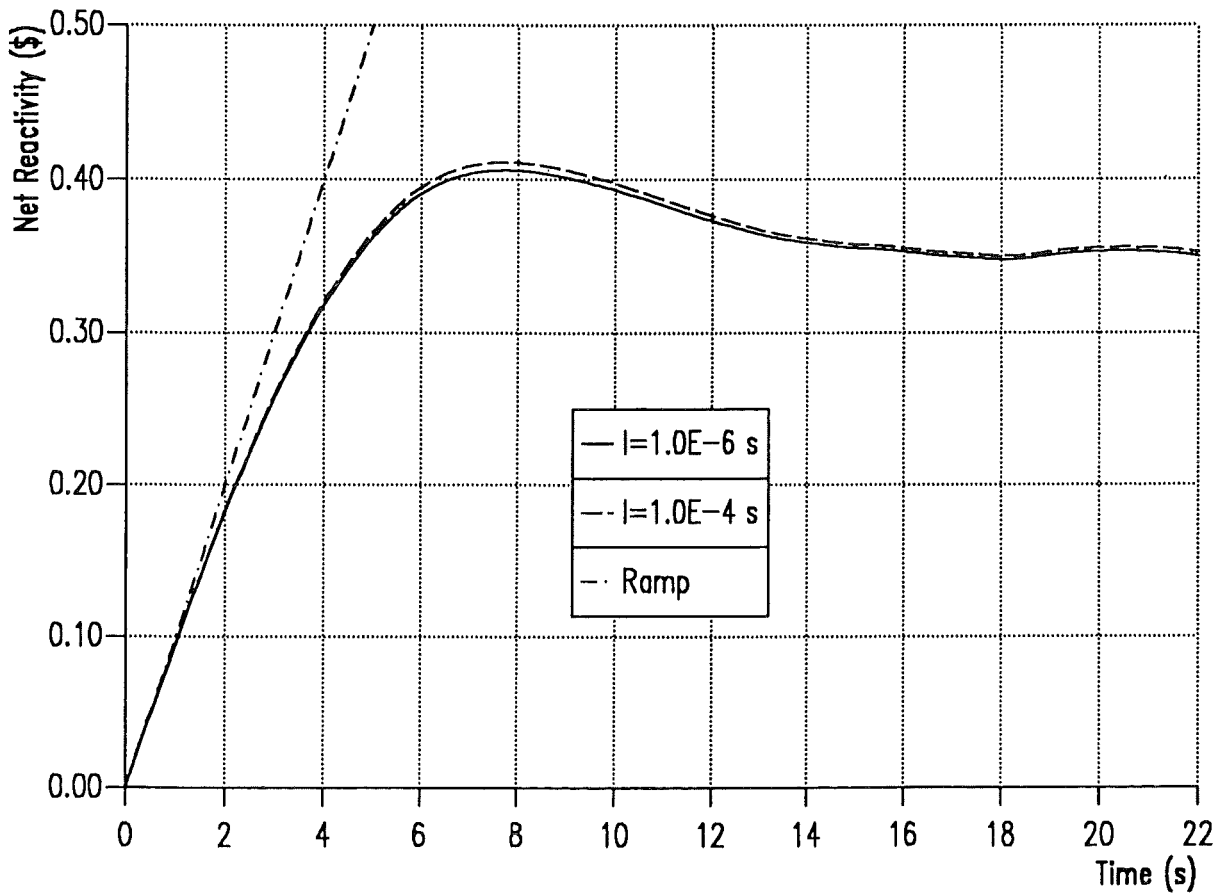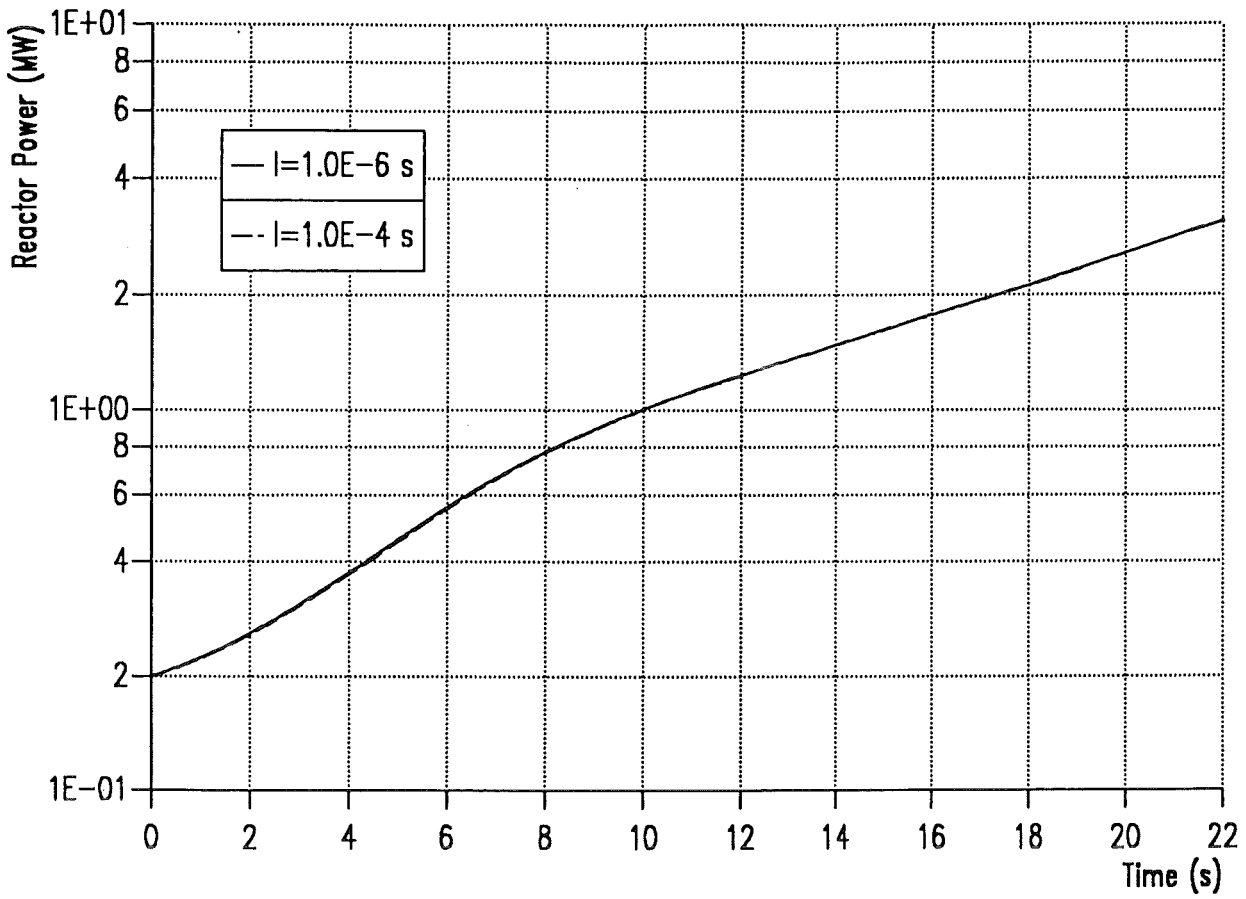
Figure 7. : Reactor power and net reactivity in ramp-induced transients from 20% of nominal power (ramp rate: 0.1 $/s) for systems with different prompt-neutron lifetimes.
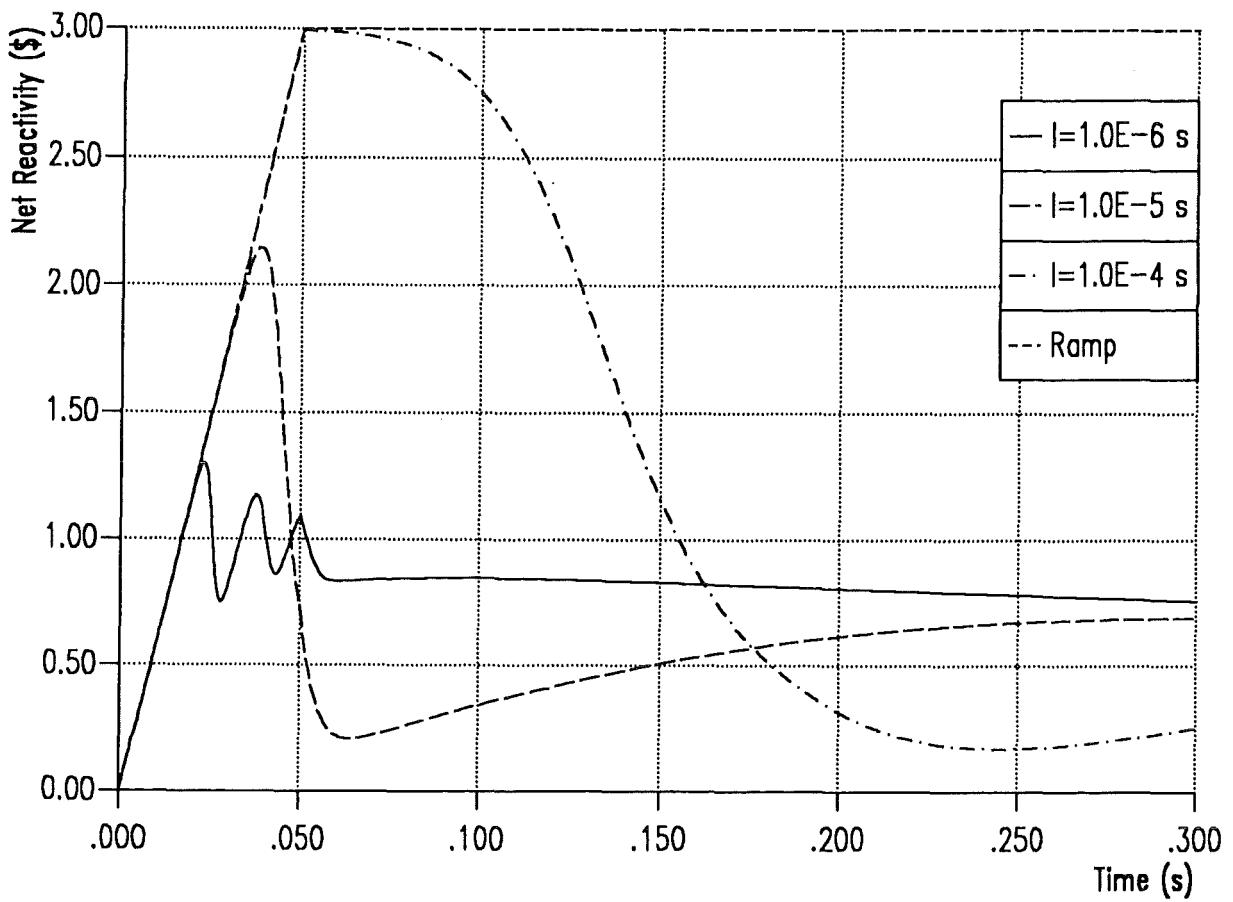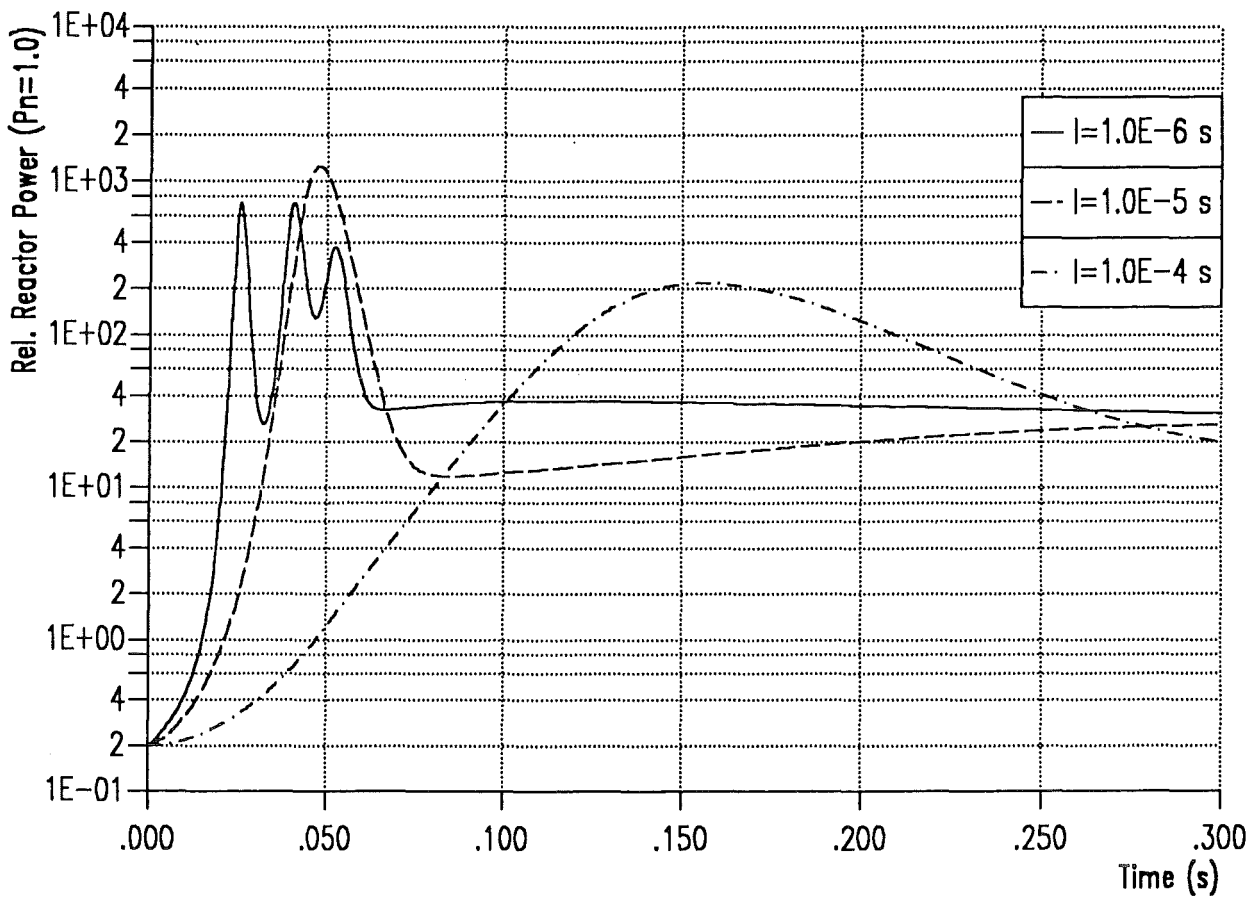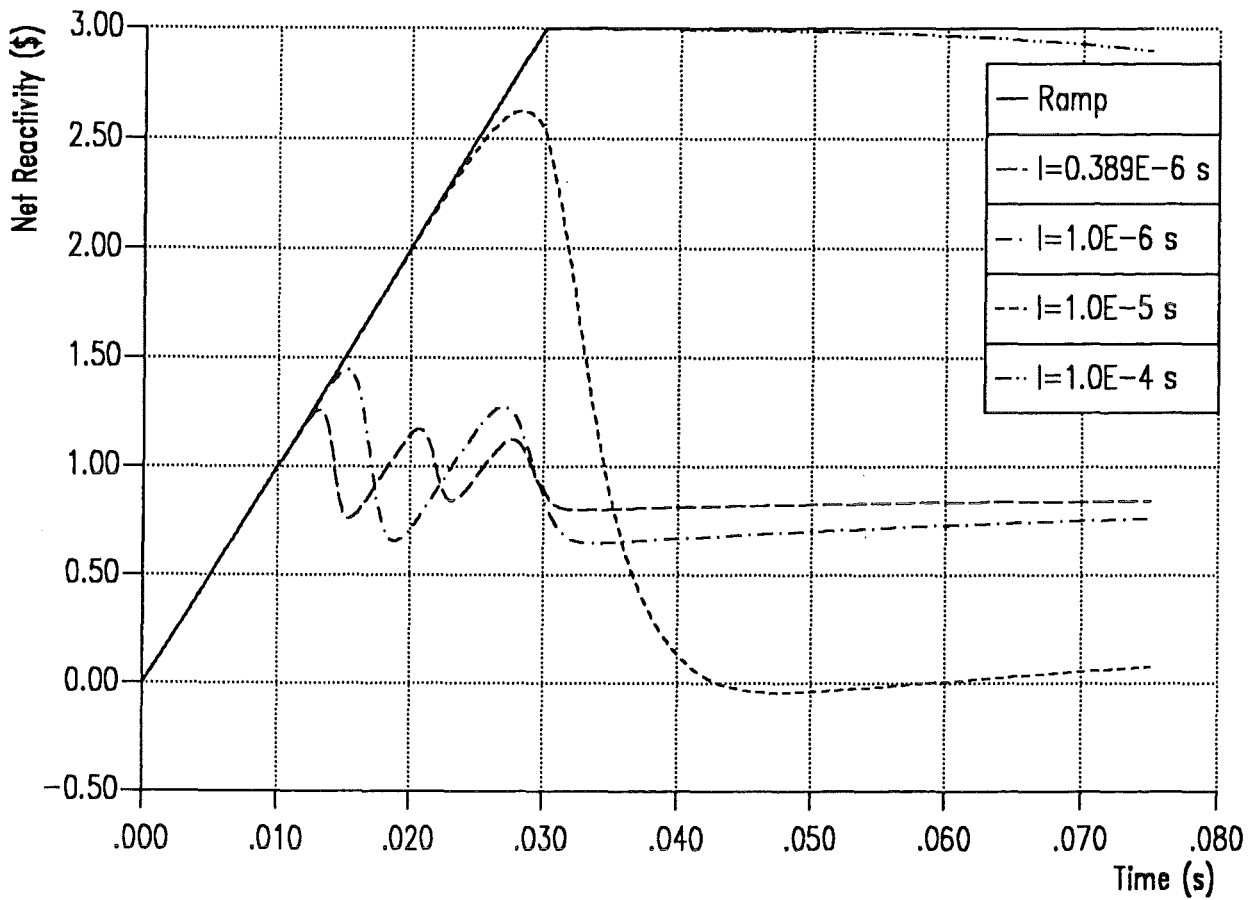
40
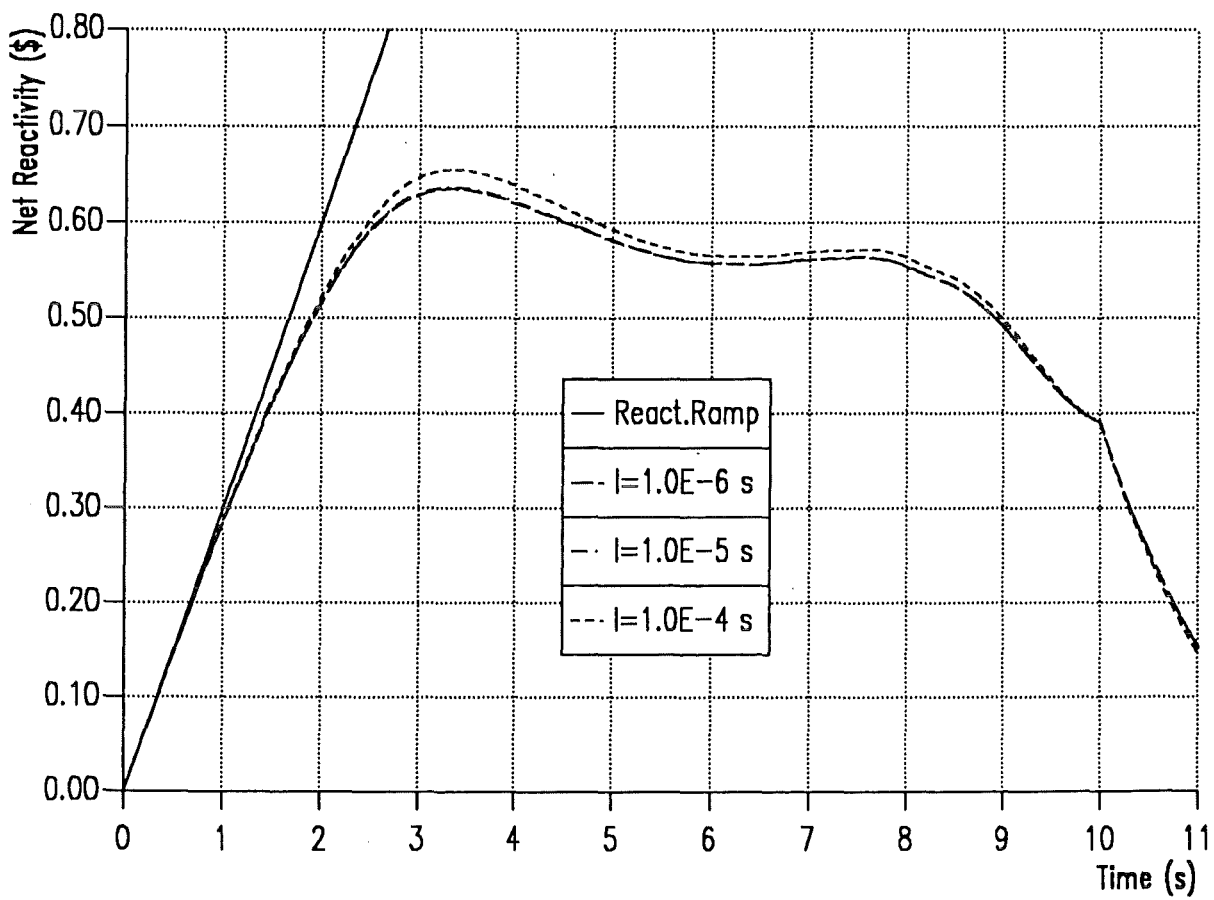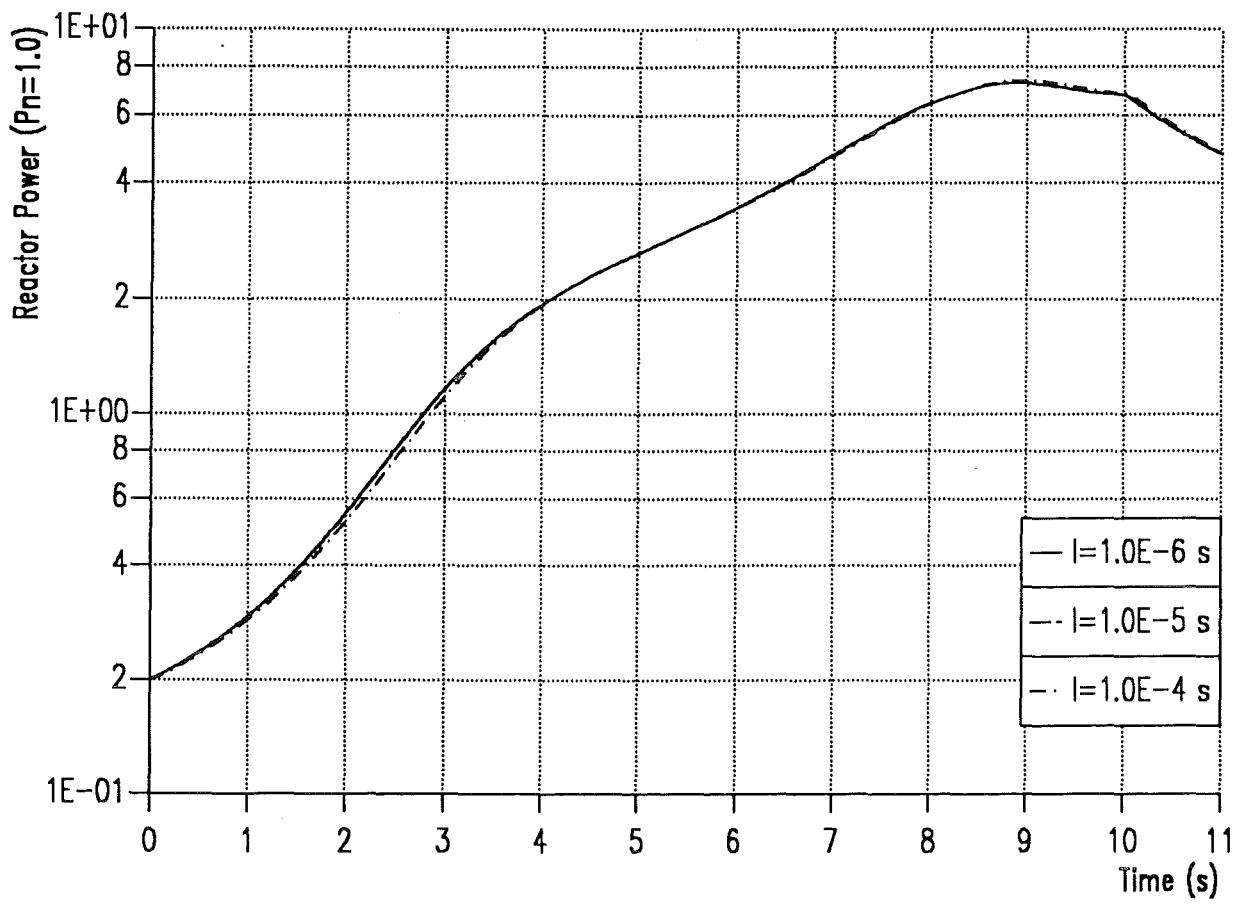
Figure 8. : Reactor power and net reactivity in ramp-induced transients from 20% of nominal power (ramp rate: 0.3 $/s) for systems with different prompt-neutron lifetimes.
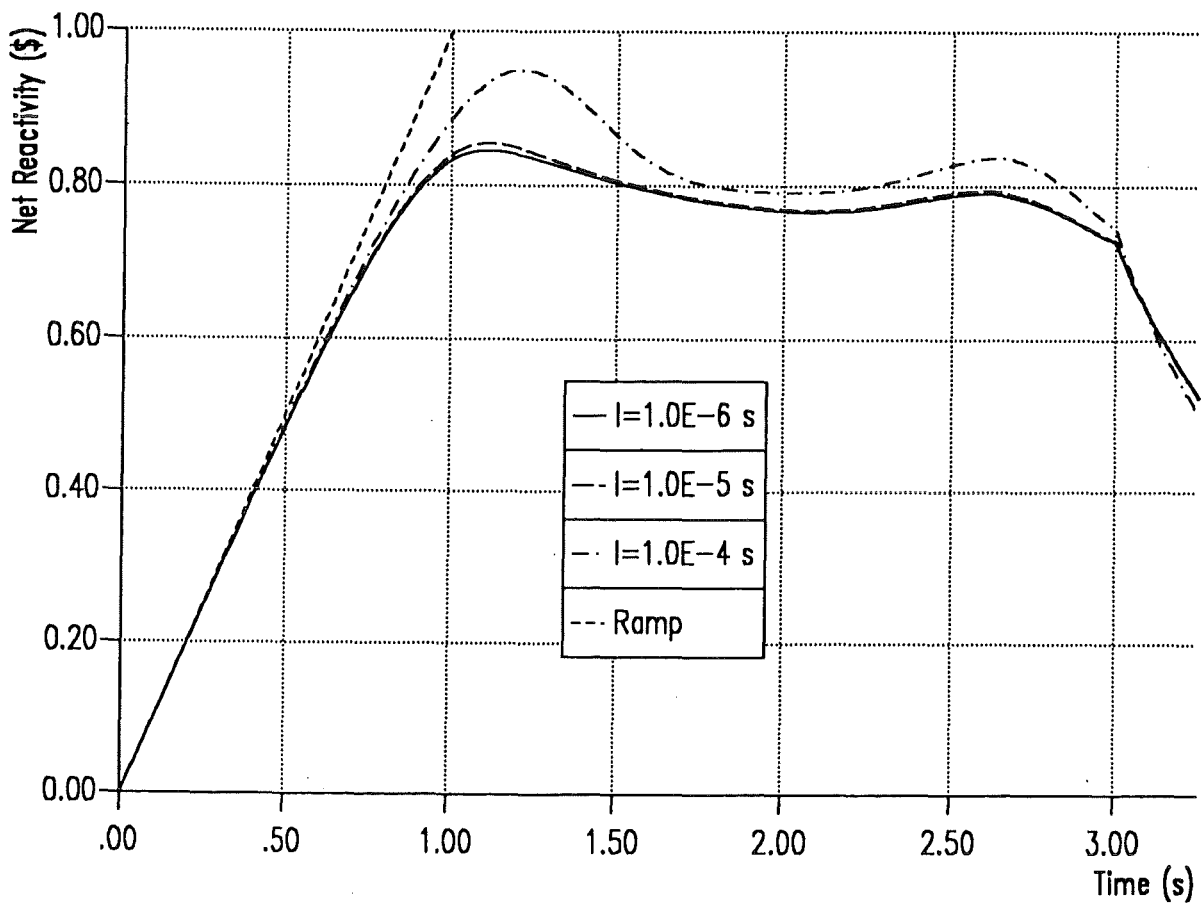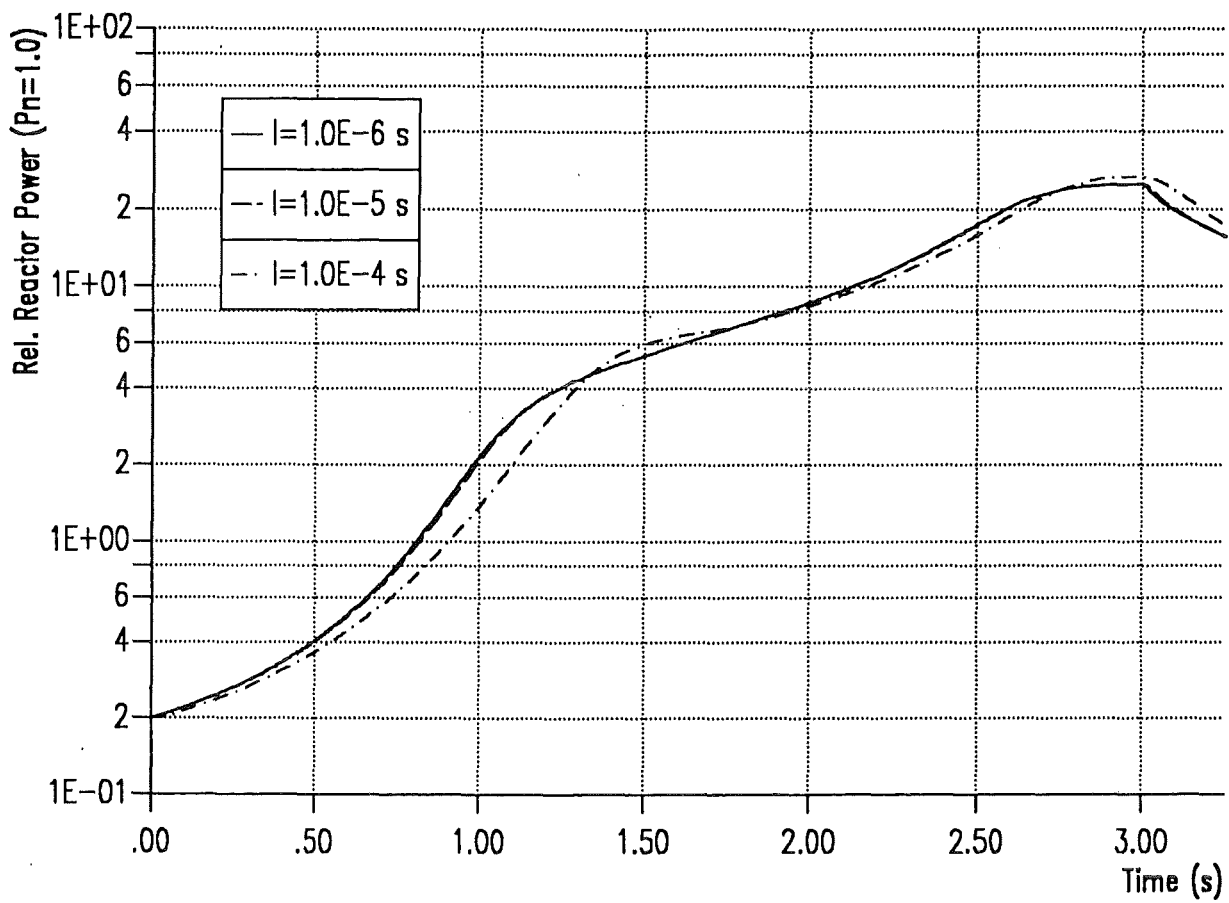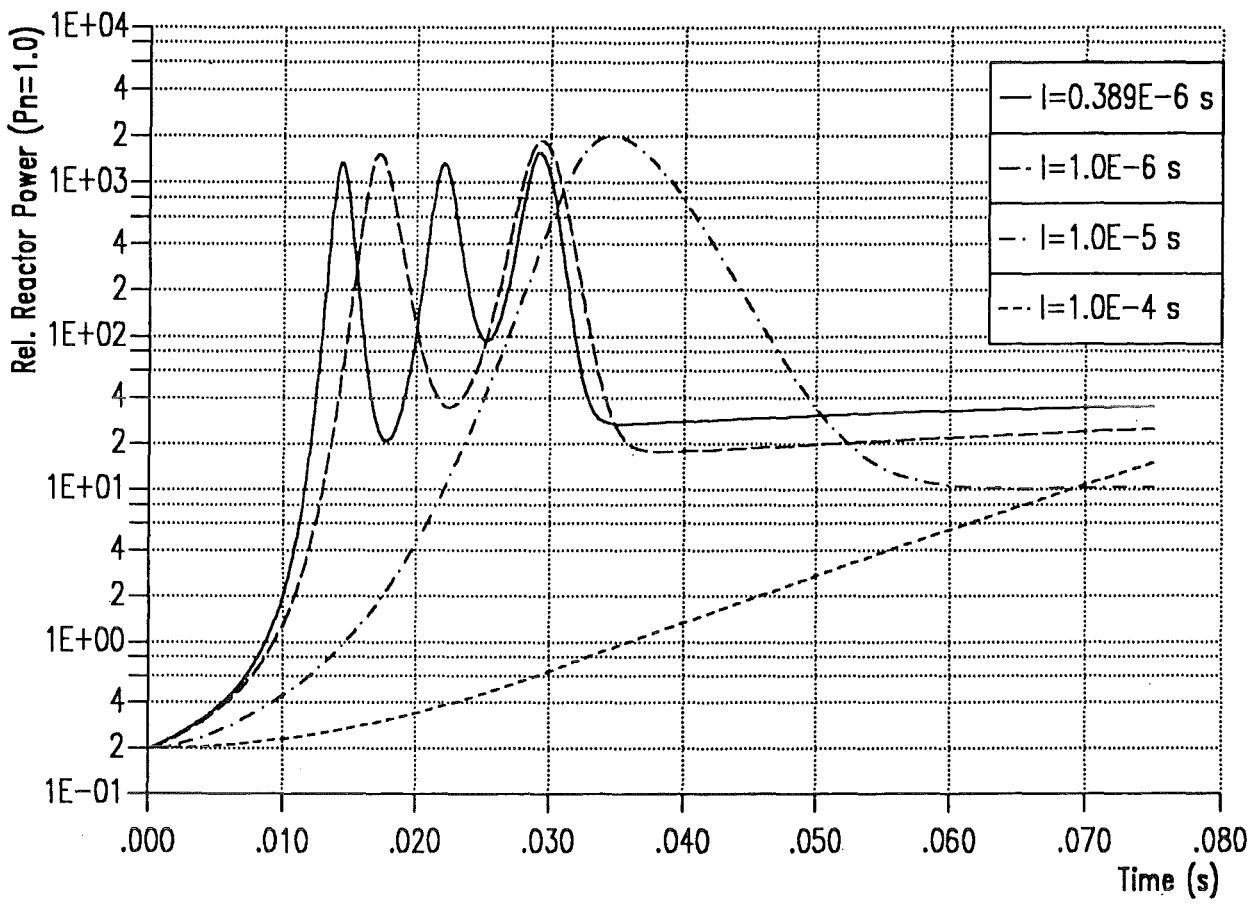
Figure 9. : Reactor power and net reactivity in ramp-induced transients from 20% of nominal power (ramp rate: 1 $/s) for systems with different prompt-neutron lifetimes.

42
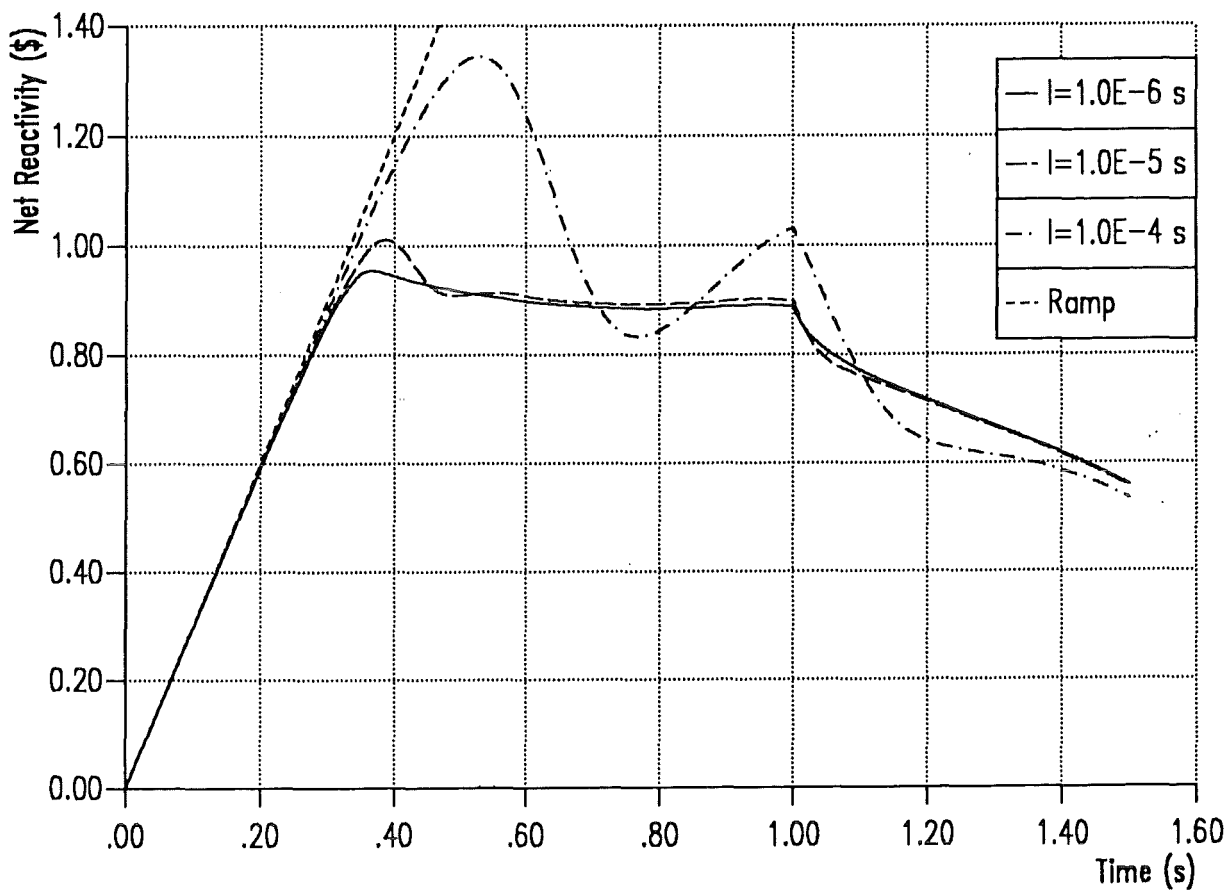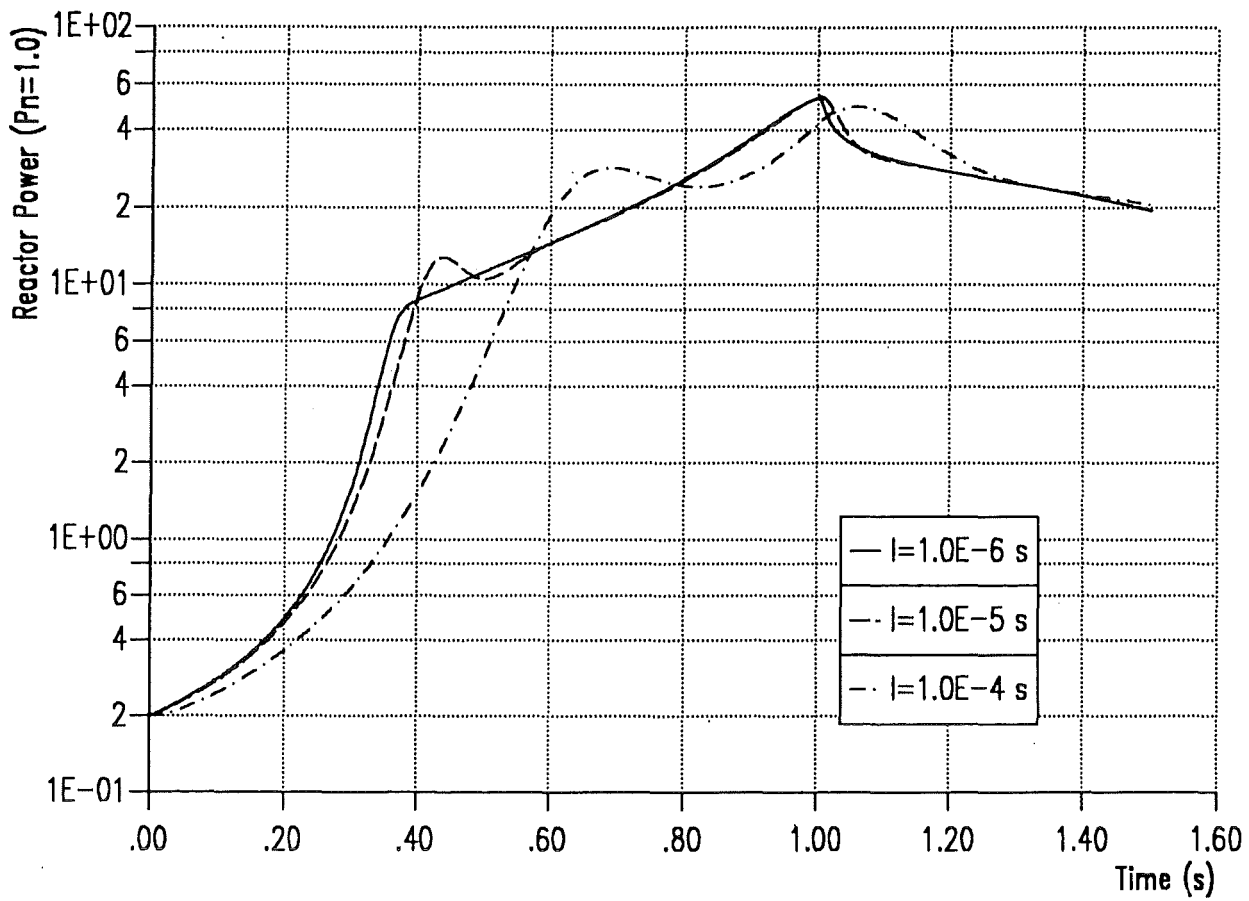
Figure 10. : Reactor power and net reactivity in ramp-induced transients from 20% of nominal power (ramp rate: 3 $/s) for systems with different prompt-neutron lifetimes.

43
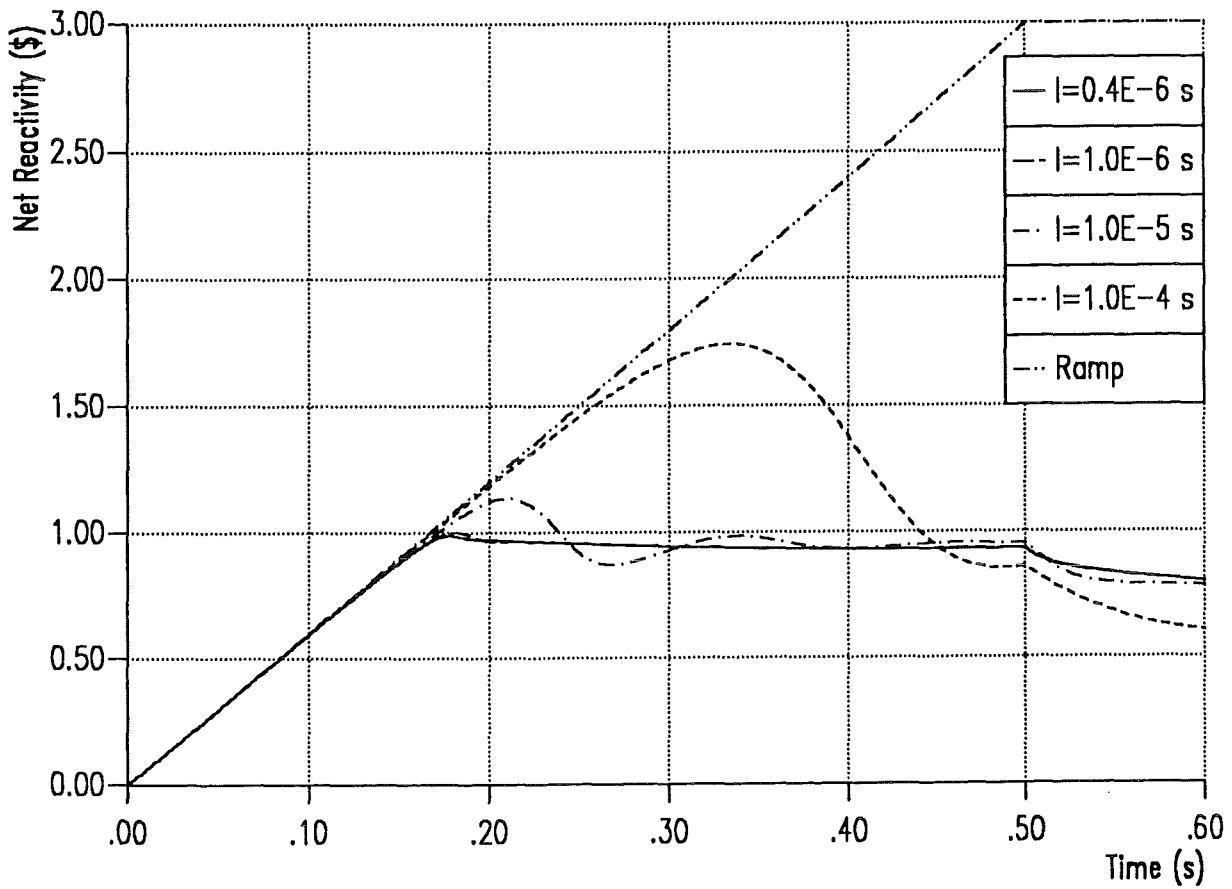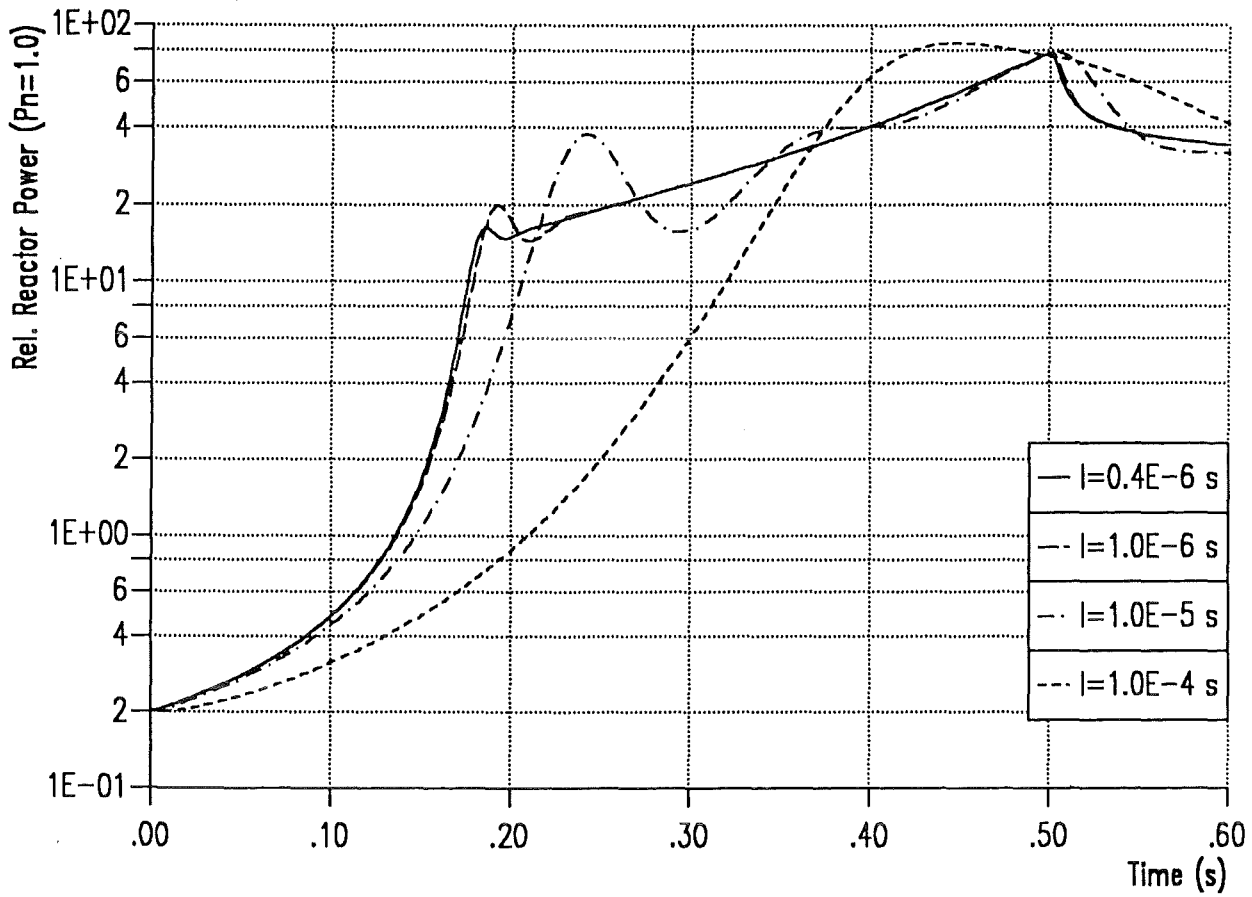
Figure 11. : Reactor power and net reactivity in ramp-induced transients from 20% of nominal power (ramp rate: 6 $/s) for systems with different prompt-neutron lifetimes.

44
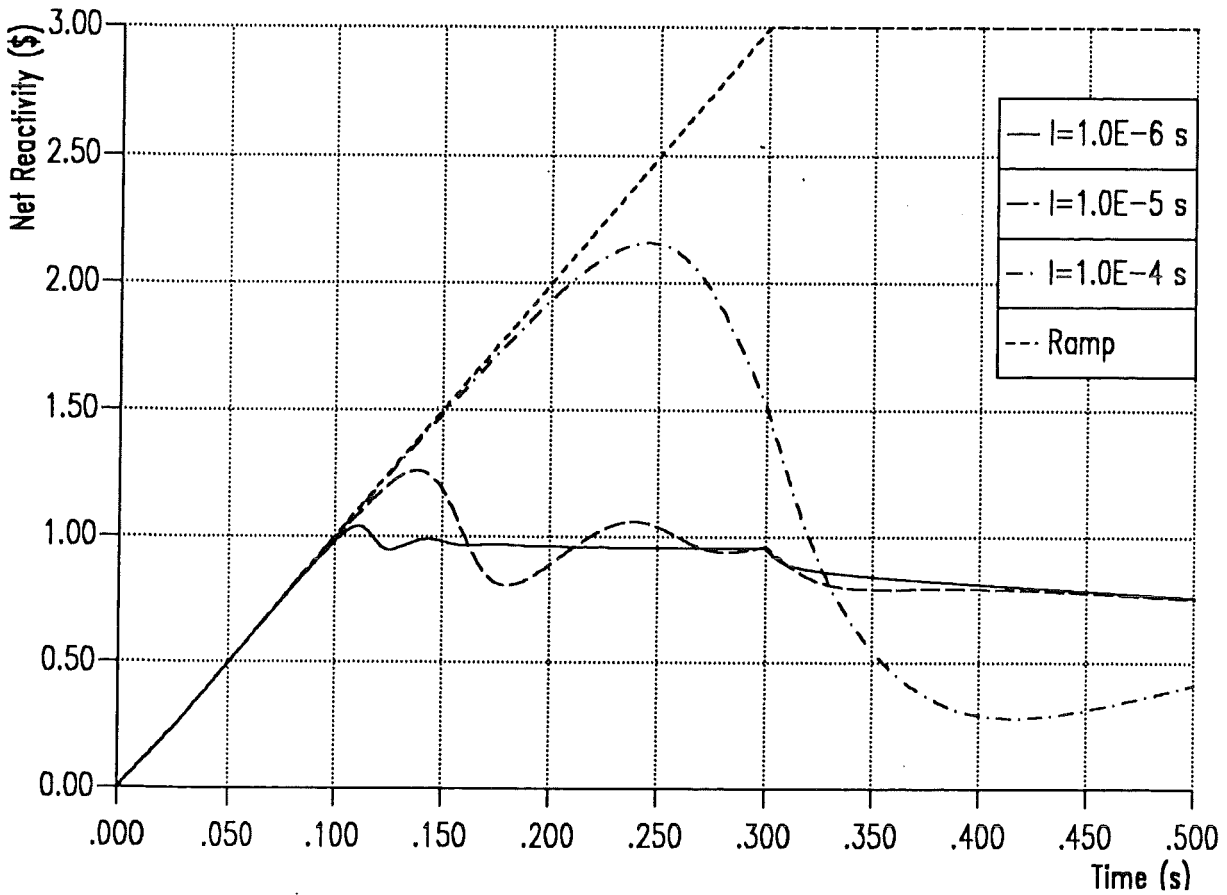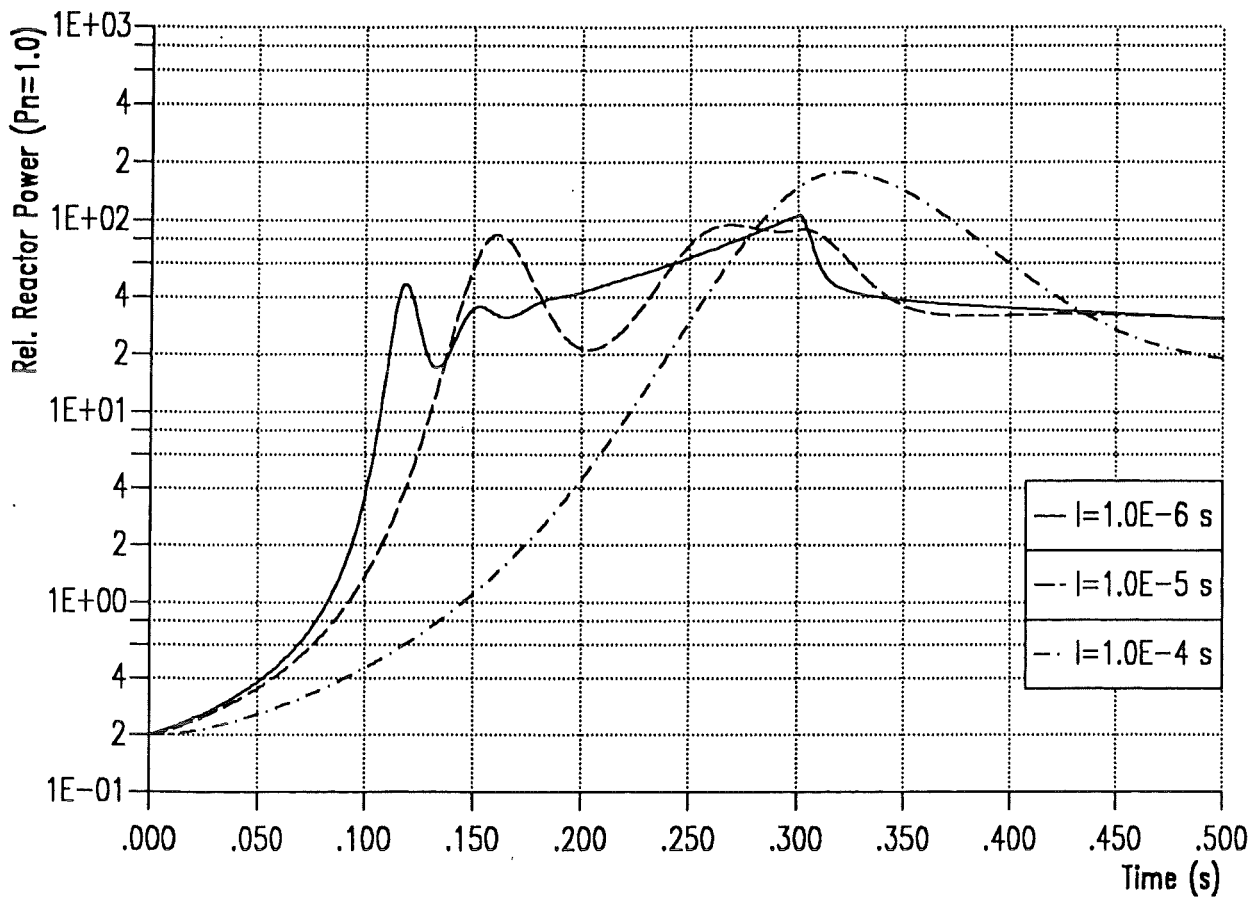
Figure 12. : Reactor power and net reactivity in ramp-induced transients from 20% of nominal power (ramp rate: 10 $/s) for systems with different prompt-neutron lifetimes.

45
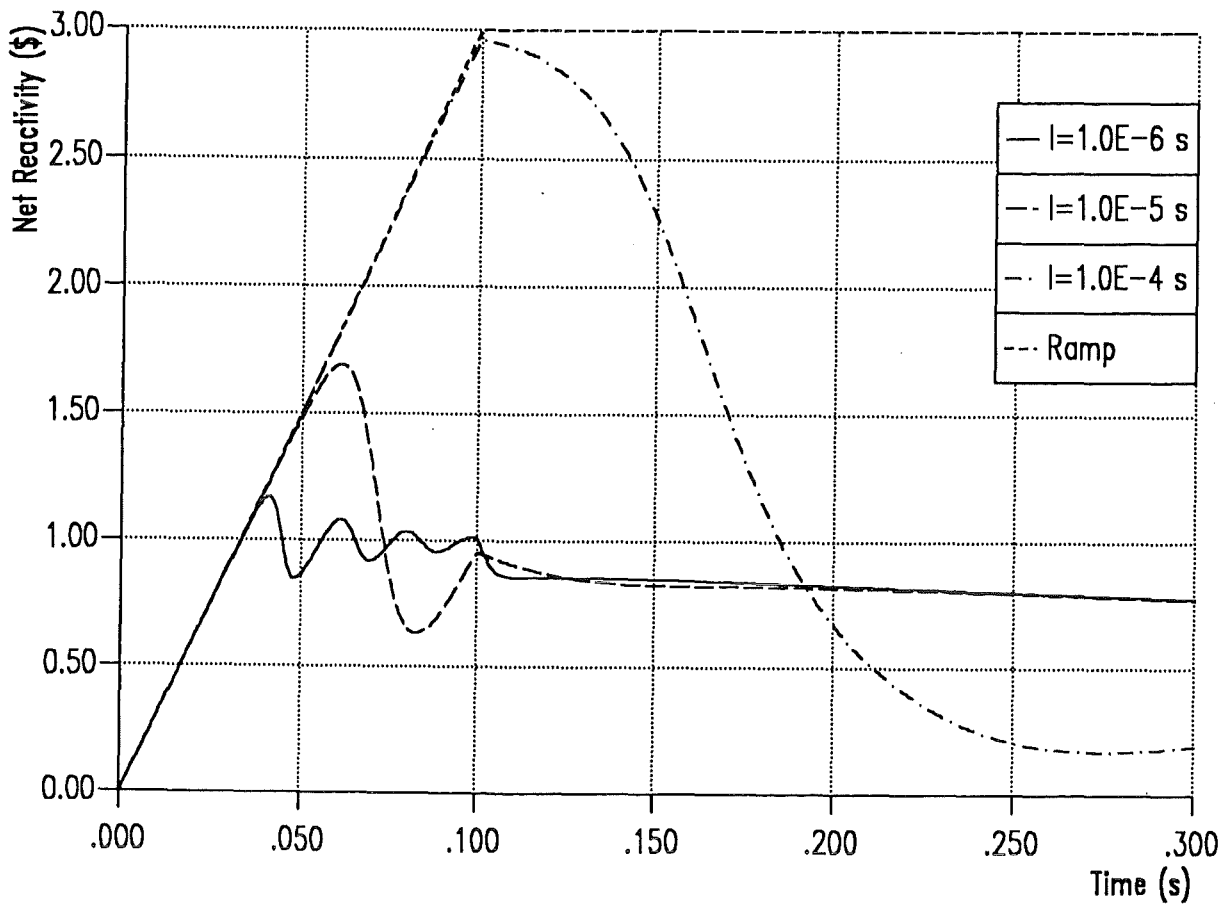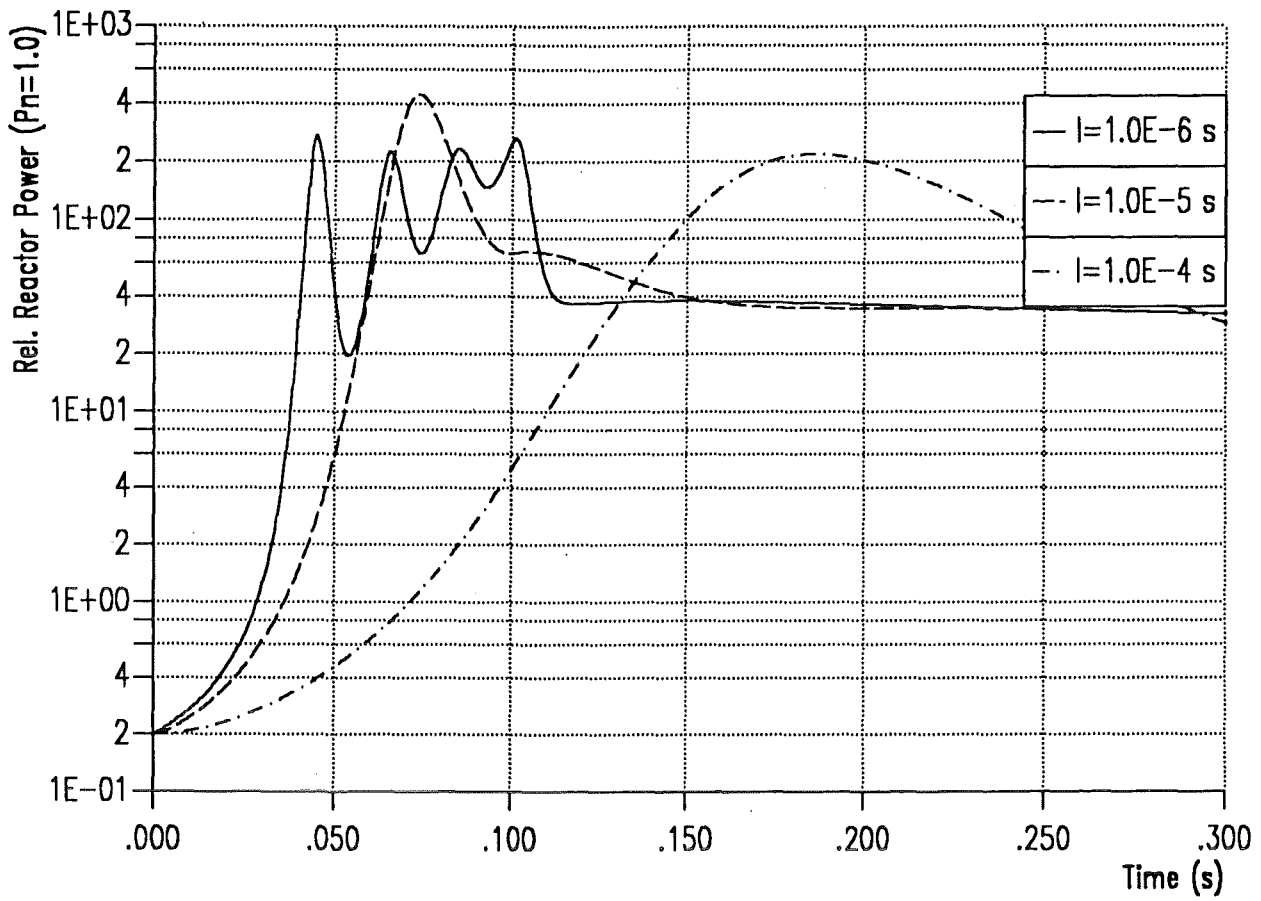
Figure 13. : Reactor power and net reactivity in ramp-induced transients from 20% of nominal power (ramp rate: 30 $/s) for systems with different prompt-neutron lifetimes.

46

Figure 14. : Reactor power and net reactivity in ramp-induced transients from 20% of nominal power (ramp rate: 60 $/s) for systems with different prompt-neutron lifetimes.

Figure 15. : Reactor power and net reactivity in ramp-induced transients from 20% of nominal power (ramp rate: 100 $/s) for systems with different prompt-neutron lifetimes.
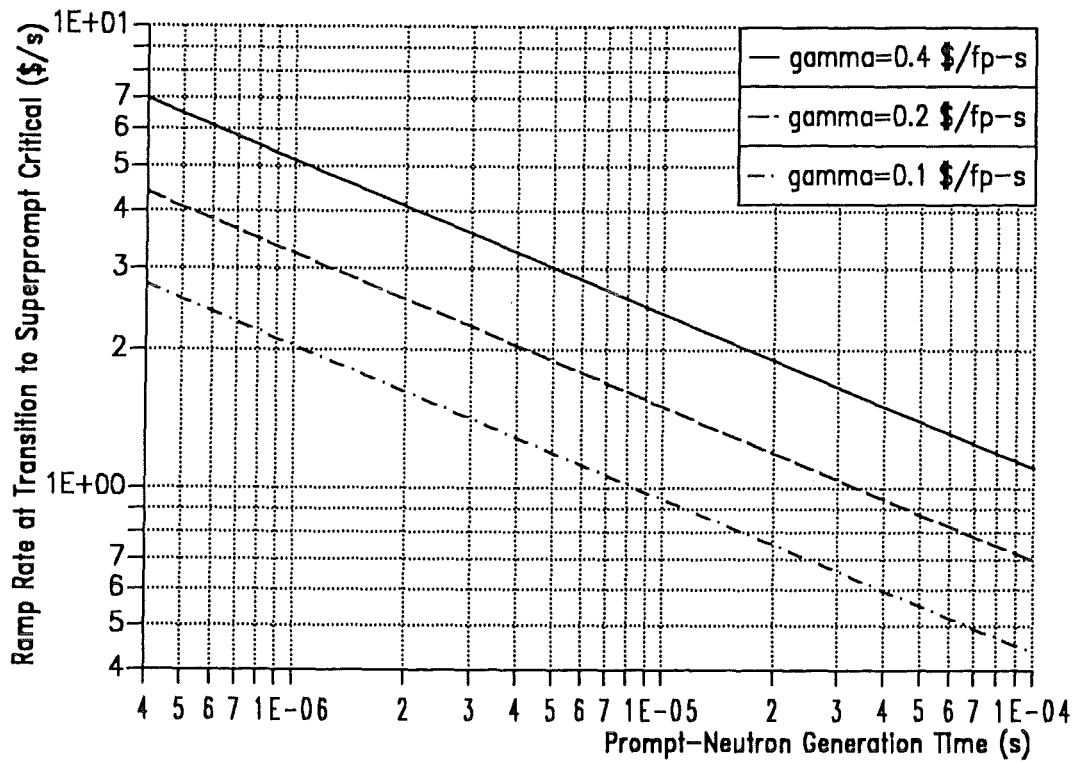
Figure 16. : Ramp rates marking the transition to prompt criticality for 3 different values of the prompt energy coefficient γ.
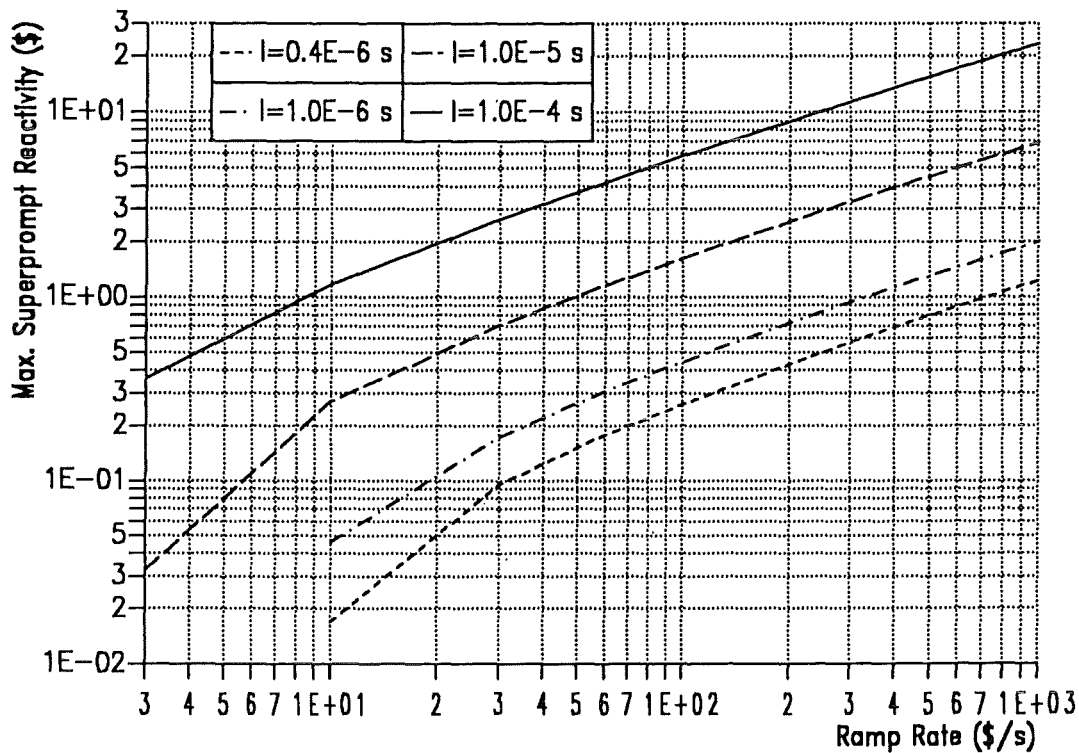
Figure 17. : Max. value of superprompt reactivity reached in transients with different ramp rates.
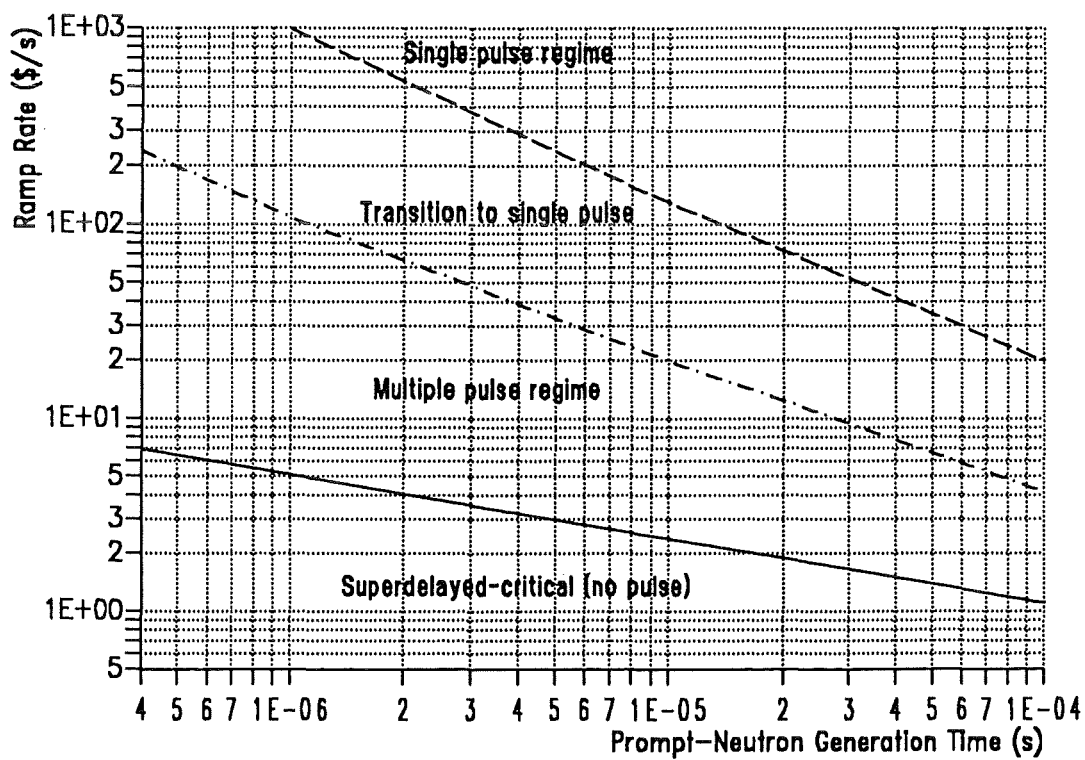
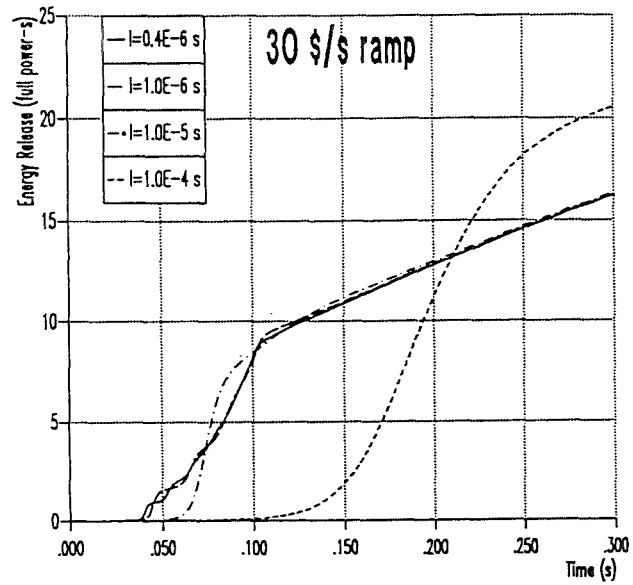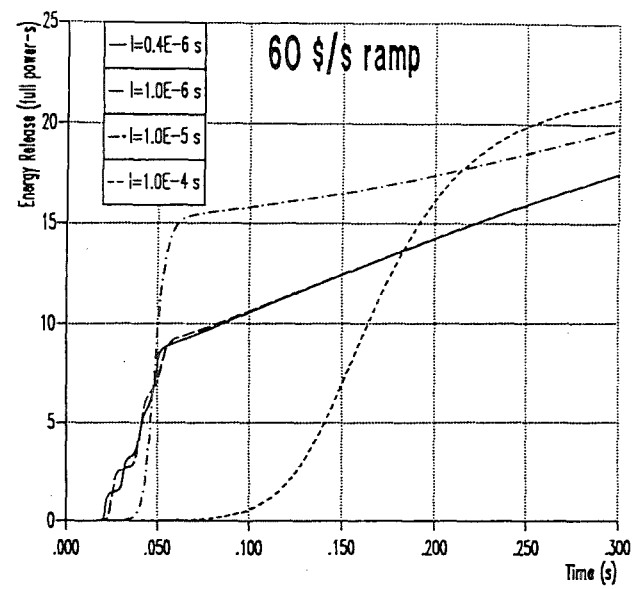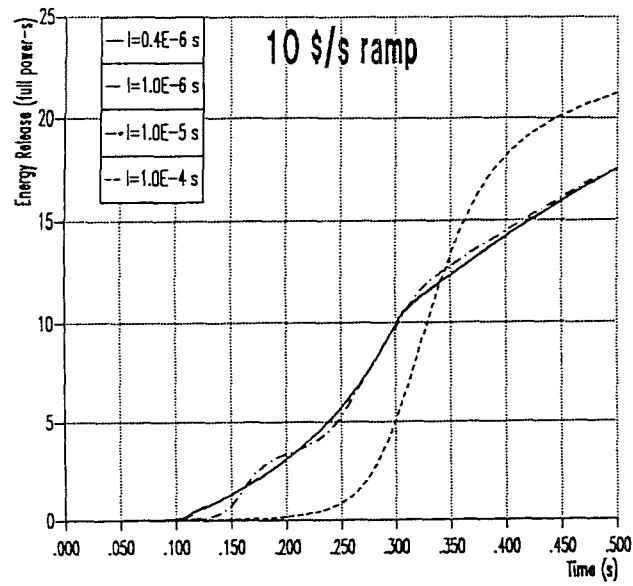**Figure 18.** : Different regimes of transients depending on ramp rate and prompt-neutron generation time.
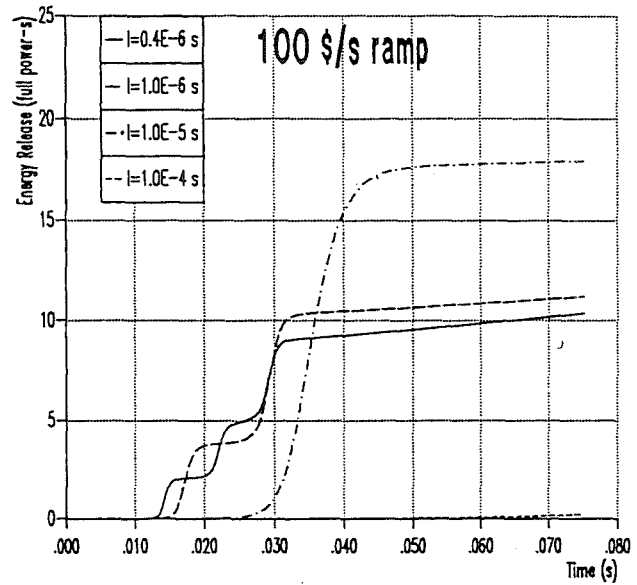
Figure 19. : Time-dependent energy release